J. Phycol. **41,** 151–176 (2005)

DOI: 10.1111/j.1529-8817.2005.04067.x

DIVERSITY IN THE GENUS *SKELETONEMA* (BACILLARIOPHYCEAE). II. AN ASSESSMENT OF THE TAXONOMY OF *S. COSTATUM*-LIKE SPECIES WITH THE DESCRIPTION OF FOUR NEW SPECIES[1]

Diana Sarno,[2] *Wiebe H. C. F. Kooistra*

Stazione Zoologica "Anthon Dohrn," Villa Comunale, 80121 Naples, Italy

Linda K. Medlin

Alfred Wegener Institute, Am Handelshafen 12, D-27570 Bremerhaven, Germany

Isabella Percopo and Adriana Zingone

Stazione Zoologica "Anthon Dohrn," Villa Comunale, 80121 Naples, Italy

The morphology of strains of *Skeletonema* Greville emend Sarno et Zingone was examined in LM, TEM, and SEM and compared with sequence data from nuclear small subunit rDNA and partial large subunit rDNA. Eight distinct entities were identified, of which four were known: *S. menzelii* Guillard, Carpenter et Reimann; *S. pseudocostatum* Medlin emend. Zingone et Sarno; *S. subsalsum* (Cleve) Bethge; and *S. tropicum* Cleve. The other four species were new: *S. dohrnii* Sarno et Kooistra sp. nov., *S. grethae* Zingone et Sarno sp. nov., *S. japonicum* Zingone et Sarno sp. nov., and *S. marinoi* Sarno et Zingone sp. nov. *Skeletonema* species fell into four morphologically distinct groups corresponding to four lineages in the small subunit and large subunit trees. Lineage I included *S. pseudocostatum*, *S. tropicum*, *S. grethae*, and *S. japonicum*. All have external processes of the fultoportulae with narrow tips that connect with those of sibling cells via fork-, knot-, or knuckle- like junctions. Lineage II included only the solitary species *S. menzelii*. Lineage III comprised *S. dohrnii* and *S. marinoi*. This latter pair have flattened and flared extremities of the processes of the fultoportulae, which interdigitate with those of contiguous valves without forming knots or knuckles. Lineage IV only contained the brackish water species *S. subsalsum*. Some species also differ in their distribution and seasonal occurrence. These findings challenge the concept of *S. costatum* as a single cosmopolitan and opportunistic species and calls for reinterpretation of the vast body of research data based on this species.

Key index words: **diatoms; diversity; LSU rDNA; morphology; new species; phylogeny; *Skeletonema*; *S. costatum*; *S. dohrnii*; *S. grethae*; *S. japonicum*; *S. marinoi*; *S. menzelii*; *S. pseudocostatum*; *S. subsalsum*; *S. tropicum*; SSU rDNA; taxonomy**

Abbreviations: **AIC, Akaike information criterion; CCAP, Culture Collection of Algae and Protozoa; CCMP, The Provasoli-Guillard National Center for Cultures of Marine Phytoplankton; FP, fultoportula; FPP, fultoportula process; hLRTs, hierarchical likelihood ratio tests; IFPP, intercalary fultoportula process; IRP, intercalary rimoportula; IRPP, intercalary rimoportula process; LSU, large subunit; ML, maximum likelihood; MP, maximum parsimony; RP, rimoportula; RPP, rimoportula process; SSU, small subunit; SZN, Stazione Zoologica "A. Dohrn" of Naples; TFP, terminal fultoportula; TFPP, terminal fultoportula process; TRP, terminal rimoportula; TRPP, terminal rimoportula process**

In 1973 Hasle wrote "To most marine planktologists, the name *Skeletonema* is synonymous with the specific name *Skeletonema costatum*." This species features in numerous research studies across all biological disciplines, and of 588 papers published since 1990 that mention *Skeletonema* in their title or abstract, 548 refer specifically to *S. costatum* (Greville) Cleve. The picture that emerges from this body of literature is of an easily culturable widely tolerant species that thrives in nutrient-rich coastal waters throughout the world. In addition, results of these different studies are interpreted and compared, with the implicit assumption that all strains and populations are part of a single species.

Skeletonema costatum is easily identified by its cylindrical cells with a ring of long processes emerging from the edge of the valve face (originally called costae by Greville [1866]). These processes are aligned parallel to the longitudinal axis of the cell and connect with similar processes of adjacent sibling valves, thus forming chains. The species was described originally as *Melosira costata* Greville (Greville 1866) and subsequently transferred to *Skeletonema* (Cleve 1873) because of the similarity of the "longitudinal costae" (processes) to those observed in the type species of that time, the

[1]Received 5 May 2004. Accepted 1 November 2004.
[2]Author for correspondence: e-mail diana@szn.it.

fossil *Skeletonema barbadensis* Greville. More recently, Sims (1994) demonstrated that several fossil *Skeletonema* species, including *S. barbadensis*, differ markedly from the extant ones. Therefore, she established a new genus, *Skeletonemopsis*, for these fossils, conserving the genus *Skeletonema* for the extant ones and with *S. costatum* as the type species (Ross et al. 1996).

After the transfer of *M. costata* to *Skeletonema* (Cleve 1873), five more species were described in the genus based on morphological characters: *S. tropicum*, *S. subsalsum*, *S. potamos* (Weber) Hasle, *S. cylindraceum* Proshkina-Lavrenko et Makarova, and *S. menzelii*. A detailed morphological investigation using EM documented considerable variation in *S. costatum* and other congeneric species (Hasle 1973). Gallagher and coworkers (Gallagher 1980, 1982, Gallagher et al. 1984) demonstrated high diversity in allozyme patterns among strains of *S. costatum* and suggested that several species might be hidden within this taxon. Medlin et al. (1991) were the first to recognize a new species, *S. pseudocostatum* Medlin, based on morphological and molecular information. However, their concept of *S. costatum* does not agree with the type and a new species must be described for it (see below).

In many areas, species attributed to *S. costatum* (*sensu lato*) are among the most important contributors to phytoplankton blooms (Karentz and Smayda 1984, Cloern et al. 1985, Estrada et al. 1985). In the Gulf of Naples, the species blooms in late spring (Ribera d'Alcalà et al. 2004), whereas in the nearby Adriatic Sea it is a recurrent winter blooming species (Zoppini et al. 1995, Totti et al. 2002, Bernardi Aubry et al. 2004). Preliminary observations revealed morphological differences between specimens obtained from these two regions, none of which completely matched any described species. These results prompted more detailed morphological and molecular analyses of several *Skeletonema* strains obtained from various places. Results of these investigations revealed previously unsuspected morphological and genetic diversity within the genus. To assess which strains belonged to *S. costatum*, a reexamination of the type material of this species was needed. The results of this study are reported in a companion article along with the description of a second species found in the type material, *S. grevillei* Sarno et Zingone (Zingone et al. 2005). None of the strains we examined here corresponds to the type material. Thus, here we describe four new *Skeletonema* species based on morphological characteristics obtained from SEM and TEM observations and differences in the nuclear-encoded small subunit (SSU) rDNA and the hypervariable region of the nuclear-encoded large subunit (LSU) rDNA.

MATERIALS AND METHODS

Isolation of strains and culture conditions. Seawater samples were collected with Niskin bottles or plankton nets in the Gulf of Naples (station MC, 40° 49′ N, 14° 15′ E) and in the Adriatic Sea on various dates (Table 1). Clonal cultures of *Skeletonema* were established from these samples by micropipette isolation. Additional strains were obtained from the Culture Collection of Algae and Protozoa (CCAP, Oban, UK), The Provasoli-Guillard National Center for Cultures of Marine Phytoplankton (CCMP, Bigelow, ME, USA), or kindly provided by colleagues mentioned in the acknowledgments. All cultures (Table 1) were maintained at the Stazione Zoologica "Anton Dohrn," Naples (SZN). *Skeletonema subsalsum* was grown in a medium prepared with 14% f/2 (Guillard 1975), 22% soil extract (1 kg garden soil boiled with 1000 mL distilled water to give 500 mL extract), and 64% bidistilled water, with a final salinity of 5 psu. All other strains were maintained in f/2 medium, adjusted to a salinity of 36 psu. Cultures were kept in glass tubes at 20–22° C and a 12:12-h light:dark cycle at 100 μmol photons $\cdot m^{-2} \cdot s^{-1}$ emitted from cool white fluorescent tubes.

Preserved material. Several natural samples from the Gulf of Naples (Tyrrhenian Sea) and the Adriatic Sea were examined to establish the morphological features of *Skeletonema* species. Tyrrhenian samples were mostly collected at station MC (see above). Adriatic samples were collected in the northern part, offshore from Venice, in winter and spring 2000–2002. A few samples collected in winter 2001 offshore of Ancona, mid-Adriatic Sea, were also examined.

LM. Light microscope observations were made on exponentially growing cultures or natural samples with an Axiophot microscope (Carl Zeiss, Oberkochen, Germany) equipped with Nomarski differential interference contrast, phase contrast, and bright-field optics. Light micrographs were taken using a Zeiss Axiocam digital camera. To remove organic matter, samples from cultures or field material were treated with acids (1:1:4, sample:HNO_3:H_2SO_4), boiled for few seconds, and then washed with distilled water. Permanent slides were prepared by mounting the dry clean material in Hyrax (Hasle 1978).

EM. Acid-cleaned material was mounted on stubs, sputter coated with gold-palladium, and observed using a Philips 505 scanning electron microscope (Philips Electron Optics BV, Eindhoven, Netherlands) or mounted onto Formvar-coated grids and observed using a Philips 400 transmission electron microscope. Fixed samples not subjected to cleaning were dehydrated in an ethanol series, critical point dried substituting 100% ethanol with CO_2, sputter coated with gold-palladium, and observed with SEM. The terminology used to describe ultrastructural features of *Skeletonema* species follows Anonymous (1975) and Ross et al. (1979).

DNA extraction, PCR, sequencing, and phylogenetic analyses. For molecular analysis, cultures of *Skeletonema* species were harvested during the exponential growth phase by centrifugation or filtration on 0.45-μm pore-size polycarbonate filters. The DNA extraction and purification, PCR amplification, sequencing, and alignment of the nuclear-encoded SSU rDNA were carried out as described in Kooistra et al. (2003) or in Medlin et al. (2000). The PCR amplification, sequencing, and alignment of the nuclear-encoded LSU rDNA were performed as described in Orsini et al. (2002). Strains used in the molecular analysis are listed in Table 1 together with the GenBank accession numbers of their SSU region and of the first approximately 800 bp of the LSU. The LSU and SSU alignments are available in the EMBL-Align database as ALIGN_000787 and ALIGN_000788, respectively. See http://www.3.ebi.ac.uk/Services/webin/help/webinalign/align_SRS_help.html

Modeltest version 3.06 (Posada and Crandall 2001) was used to select optimal base substitution models and values for base composition,% invariable sites, and gamma shape parameter according to hierarchical likelihood ratio tests (hLRTs) and Akaike information criterion (AIC). Maximum likelihood (ML) analyses of the alignment were performed under the full heuristic search option in PAUP* version 4.0b10 (Swofford 2002) and were constrained with values obtained by Modeltest.

TABLE 1. Strains used in the analyses and corresponding GenBank accession numbers.

Species	Strain designation	Isolation site	Isolation date	GenBank accession number (SSU)	GenBank accession number (LSU)
Skeletonema dohrni	SZN-B104	Gulf of Naples, South Tyrrhenian, Mediterranean Sea	4 Feb. 2002	AJ632210	AJ633537
	SZN-B105	Gulf of Naples, South Tyrrhenian, Mediterranean Sea	11 Feb. 2002	AJ632211	AJ633538
	SZN-B191	Gulf of Naples, South Tyrrhenian, Mediterranean Sea	5 Feb. 2004		As SZN-B105
Skeletonema grethae	SZN-B190	Indian River Lagoon, Florida, North Atlantic Ocean			AJ633523
	CCAP1077/3[a]	Narragansett Bay, North Atlantic Ocean	Oct. 1986	AJ632204 X85395[f,g]	AJ633521
	CCMP780[b]	Nantucket Sound, North Atlantic Ocean	1974	AJ632205	AJ633522
	UBC18/C	Georgia Strait, North Pacific Ocean		M54988.1[f,g]	
Skeletonema japonicum	SZN-B149	Hiroshima Bay, Seto Inland Sea, North Pacific Ocean	Oct. 2002		AJ633524
Skeletonema marinoi	SZN-B118	North Adriatic, Mediterranean Sea	22 Feb. 2002	AJ632214	AJ633530
	SZN-B119	North Adriatic, Mediterranean Sea	22 Feb. 2002	AJ632215	AJ633531
	SZN-B120	North Adriatic, Mediterranean Sea	22 Feb. 2002	AJ632216	AJ633532
	SZN-B121	North Adriatic, Mediterranean Sea	22 Feb. 2002	AJ632212	AJ633533
	SZN-B146	North Adriatic, Mediterranean Sea	22 Feb. 2002	AJ632213	AJ633534
	SZN-B147	North Adriatic, Mediterranean Sea	22 Feb. 2002		AJ633535
	SZN-B189	Hong Kong, South China Sea, North Pacific Ocean	Summer 2001		AJ633529
	CCMP1009[c]	North America, Atlantic Ocean	1977	AJ535165[h,i]	AJ633536
	Lange			AF462060.1[f,j]	
Skeletonema menzelii	SZN-B82	Gulf of Naples, South Tyrrhenian, Mediterranean Sea	18 Dec. 2001	AJ632217	AJ633526
	SZN-B83	Gulf of Naples, South Tyrrhenian, Mediterranean Sea	18 Dec. 2001	AJ632218	AJ633525
	CCMP790	Gulf of Maine, North Atlantic Ocean		AJ535168[f]	AJ633528
	CCMP787[d]	Sargasso Sea, North Atlantic Ocean		AJ536450[f]	AJ633527
Skeletonema pseudocostatum	SZN-B77	Gulf of Naples, South Tyrrhenian, Mediterranean Sea	29 May 2001	AJ632207	AJ633507
	SZN-B78	Gulf of Naples, South Tyrrhenian, Mediterranean Sea	18 Dec. 2001	AJ632208	AJ633508
	SZN-B79	Gulf of Naples, South Tyrrhenian, Mediterranean Sea	8 Jan. 2002		AJ633509
	SZN-B80	Gulf of Naples, South Tyrrhenian, Mediterranean Sea	21 Jan. 2002	AJ632209	AJ633510
	SZN-B81	Gulf of Naples, South Tyrrhenian, Mediterranean Sea	29 Jan. 2002		AJ633511
	SZN-B139	Gulf of Naples, South Tyrrhenian, Mediterranean Sea	12 Mar. 2002		AJ633512
	SZN-B140	Gulf of Naples, South Tyrrhenian, Mediterranean Sea	20 May 2002		AJ633513
	CCAP1077/7	Alexandria, Egypt, Mediterranean Sea	Dec. 1983	X85394[h]	AJ633514
	CCAP1077/6[e]	Australia, South Pacific Ocean	Jul. 1978	X85393[f]	
	Unknown				Y11512[f]
Skeletonema subsalsum	CCAP1077/8	Lough Erne, Ireland, North Atlantic Ocean	1991	AJ535166[f]	AJ633539
Skeletonema tropicum	SZN-B141	Gulf of Naples, South Tyrrhenian, Mediterranean Sea	3 Oct. 2002		AJ633515
	SZN-B142	Gulf of Naples, South Tyrrhenian, Mediterranean Sea	3 Oct. 2002		AJ633516
	SZN-B143	Gulf of Naples, South Tyrrhenian, Mediterranean Sea	12 Nov. 2002		AJ633517
	SZN-B144	Gulf of Naples, South Tyrrhenian, Mediterranean Sea	12 Nov. 2002		AJ633518
	SZN-B145	Gulf of Naples, South Tyrrhenian, Mediterranean Sea	12 Nov. 2002		AJ633519
	CCMP788	Gulf of Mexico, North Atlantic Ocean	1973		AJ633520
Detonula confervacea				AF525672[f]	
Lauderia annulata				X85399[f]	
Thalassiosira sp. 1	CCMP1281			AJ535171[f]	
Thalassiosira sp. 2	SZN-B101				AJ633506
T. eccentrica				X85396[f]	
T. profunda		Monterey Bay, California, North Pacific Ocean		As SZN-B105	
T. pseudonana				AJ535169[f]	
T. rotula	CCAP1085/4			X85397[f]	AJ633505[f]
Porosira pseudodenticulata				X85398[f]	
Bellerochea malleus				AF525670[f]	
Ditylum brightwellii				X85386[f]	
Helicotheca tamesis				X85385[f]	
Lithodesmium undulatum				Y10569[f]	

[a]Labeled in CCAP as *S. costatum*.
[b]Labeled in CCMP as *S. costatum*.
[c]Labeled in CCMP as *S.* cf. *subsalsum*.
[d]As Men 5 in Guillard et al. (1974).
[e]As CS76 in Medlin et al. (1991).
[f]Sequence obtained from GenBank.
[g]Labeled in GenBank as *S. costatum*.
[h]Sequence obtained from GenBank, also sequenced at SZN with identical results.
[i]Labeled in GenBank as *S.* sp.
[j]Labeled in GenBank as *S. pseudocostatum*.

Identical sequences were removed before data analysis to minimize calculation time. Bootstrap values (1000 replicates) were calculated using the same ML model, but in case a clade contained only identical sequences, two were retained instead of one to permit calculation of the support for that clade. Maximum parsimony (MP) analyses were carried out using full heuristic searches also using PAUP*. The SSU data set contained 36 sequences and 1824 positions; the LSU data set contained 37 sequences and 796 positions.

RESULTS AND DISCUSSION

Morphology. Eight distinct morphs were identified, none of which corresponded to the morphology of

the type material of *S. costatum* (Zingone et al. 2005). Four were attributable to already described species, viz., S. *menzelii*, *S. pseudocostatum*, *S. subsalsum*, and *S. tropicum*. An emended description was warranted for *S. pseudocostatum*, and additional morphological features were observed in the other three species. The other four morphs constitute new species. Two of these, *S. dohrnii* and *S. marinoi*, were isolated from the Mediterranean Sea, whereas *S. japonicum* was identified in a strain from the Seto Inland Sea (Japan). The fourth new species, *S. grethae*, was established for material identified as *S. costatum* in a previous article (Medlin et al. 1991). Morphometric and morphological characteristics of all the species examined are summarized in Tables 2 and 3, respectively.

Skeletonema Greville emend. Sarno et Zingone (Fig. 1, A–N)

Cells cylindrical in shape, colonial or solitary. Each cell contains one, two, or many chloroplasts. Valve diameter 2–38 μm. Valves flattened or slightly convex, valve mantle almost perpendicular. Costae emerging from a circular annulus, delimiting radial rows of poroid or pseudoloculate areolae, 26–58 in 10 μm. Fultoportulae (FPs) located in a marginal ring, with two or three satellite pores. External processes of the FPs generally long and tubular, open or closed along their length. The processes are oriented perpendicularly to the valve face, and their ends join with those of the processes of contiguous valves, each connecting to one or two opposite processes. Each valve possesses a single rimoportula (RP), located marginally in intercalary valves and subcentrally or marginally in terminal valves. The tubular process of the RP is long in terminal valves, whereas it can be short or long in intercalary valves. Cingulum formed of a valvocopula and several open bands with ligula and antiligula. Each copula has a central longitudinal ridge on either side of which are transverse ribs (11–16 in 1 μm) interspaced by uniseriate rows of pores or by smooth hyaline areas.

Description: The general morphological features of *Skeletonema* species examined in this investigation (Fig. 1) generally coincide with those illustrated in previous descriptions of the genus (Castellví 1971, Hasle 1973, Round 1973, Housley et al. 1975, Fryxell 1976, Smith 1981, Round et al. 1990). With the exception of *S. menzelii*, all form colonies of variable length, generally straight, sometimes curved or coiled (Fig. 1A). The cells are cylindrical, with a more or less convex valve surface, and the mantle is slightly oblique or perpendicular to the valve face (Fig. 1, C, E, G, and I). In our material, cell diameter ranges between 2 and 17.5 μm, more often 4–8 μm. Specimens of larger size (<38 μm diameter) are reported in the literature (Cleve 1900, Hasle 1973); the pervalvar axis length is variable depending on the extension of the cingulum.

Each cell generally contains one to two parietal chloroplasts except for *S. cylindraceum*, *S. japonicum*, and *S. tropicum*, which may have several chloroplasts. In most species, radial and tangential costae run across the valve in a network, delimiting radial rows of areolae (Fig. 1B). The areolae are quadrangular or irregularly circular, but those located at the branching points of the network may be triangular. The radial costae originate from a central annulus (Fig. 1B), which may contain a variable number of irregular areolae. The costae are generally thicker toward the valve margin and on the mantle, where the areolae become pseudoloculate. The areolae are occluded by an internal cribrum perforated by minute pores. Transverse costae and areolae are missing in *S. menzelii* thus this species has only a basal siliceous layer.

The FPs, or strutted processes, are located in a marginal ring at the transition between the valve face and the mantle (Fig. 1, B–J). Three satellite pores lie at the base of each FP in all species (Fig. 1B), with the exception of *S. menzelii*, which has two satellite pores. In some cases, thin organic fibers are seen to emerge from the FPs in culture material (Castellví 1971, Yamada and Takano 1987). Each FP is associated with a long external process (fultoportula process, FPP) oriented parallel to the pervalvar axis and aligned perfectly with the surfaces of the cingulum and mantle (Fig. 1, A and C–J). The FPPs are generally semicircular in cross-section with an external split along their length. The margins of the split may coalesce partially (*S. tropicum*) or along the whole length (*S. costatum*, *S. subsalsum*), leaving a proximal opening or a pore, respectively, and often showing a suture along the fusion line. In other cases (*S. pseudocostatum*, *S. japonicum*) the base of the FPP is tubular in terminal cells of the colonies. The processes are variable in length within species depending on culture conditions, smallest in *S. subsalsum*, where they can also completely occlude the peripheral space between sibling valves.

Process shape differs among the species and also between intercalary and terminal valves of the colony in individual species. In the following, "terminal fultoportula (TFP)" and "intercalary FP" are used to designate the FPs of terminal and intercalary valves of the colonies, respectively, whereas "terminal fultoportula process (TFPP)" and "intercalary fultoportula process (IFPP)" are used to designate the external projections of the FPs of the terminal (Fig. 1, C–F) and intercalary valves (Fig. 1, G–J) of the colonies, respectively. TFPPs generally have either flared or narrow tips (Fig. 1, C and E), which can be distinguished in LM (Fig. 1, D and F). The TFPP tips can be truncated, jagged, or have spines, finger-, or claw-shaped projections. In some cases, IFPPs of sibling valves are aligned, each joining a single IFPP of the next cell (1:1 junction), with a visible thickening at the junction (Fig. 1, G and H). In other cases the IFPPs are displaced, one IFPP joining two IFPPs of the next cell (1:2 junction). When the displacement and the 1:2 junction are encountered along the whole ring of IFPPs (Fig. 1I), a transverse zigzag (serrated teeth) line may be seen in LM (Hasle 1973) (Fig. 1J). Sibling valves do not separate upon acid cleaning.

Each valve bears a single RP or labiate process (Fig. 1, B, C, E, and G) with an external tubular process, the

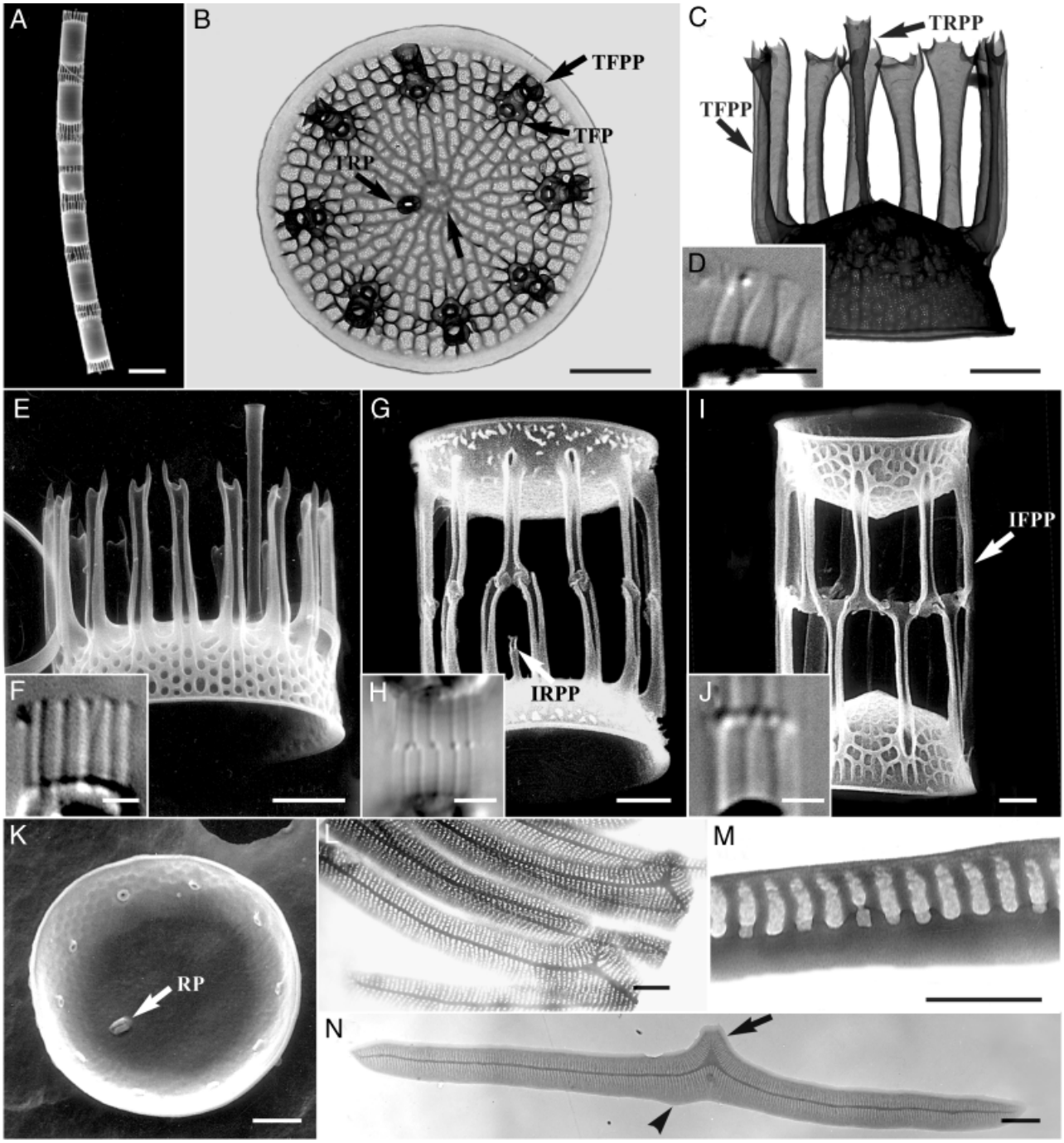

FIG. 1. General morphology of the genus *Skeletonema*. LM: D, F, H, and J; SEM: A, E, G, I, and K; TEM: B, C, and L–N. (A) *Skeletonema marinoi*, strain SZN-B121, colony in girdle view. Scale bar, 10 µm. (B) *Skeletonema pseudocostatum*, strain SZN-B80, terminal valve in valve view with the TRP, the annulus (arrow), the TFPs, and the TFPPs. Note the three satellite pores at the base of the FPs. Scale bar, 1 µm. (C) *Skeletonema dohrnii*, strain SZN-B105, terminal valve in girdle view, with the TFPPs and the TRPP. Scale bar, 1 µm. (D) *Skeletonema dohrnii*, strain SZN-B191, terminal valve with the TFPPs. Scale bar, 2 µm. (E) *Skeletonema tropicum*, strain SZN-B142, terminal valve with the TFPPs and the TRPP. Scale bar, 2 µm. (F) *Skeletonema grethae*, strain SZN-B190, terminal valve with the TFPPs. Scale bar, 2 µm. (G) *Skeletonema tropicum*, strain SZN-B141, intercalary valves in girdle view, with the IFPPs, joined in a 1:1 fashion. Note a single IFPP joined to two opposite IFPPs. The arrow shows the IRPP. Scale bar, 2 µm. (H) *Skeletonema tropicum*, strain SZN-B144, intercalary valves. Scale bar, 5 µm. (I) *Skeletonema japonicum*, strain SZN-B149, intercalary valves in girdle view, with IFPPs joined in a 1:2 fashion. Scale bar, 1 µm. (J) *Skeletonema dohrnii*, strain SZN-B191, intercalary valves. Scale bar, 2 µm. (K) *Skeletonema subsalsum*, strain SZN-B114, internal view of a terminal valve. Note the RP, appearing as a slit with two lips. Scale bar, 1 µm. (L) *Skeletonema marinoi*, strain SZN-B120, cingular bands. Scale bar, 1 µm. (M) *Skeletonema pseudocostatum*, strain SZN-B77, valvocopula. Scale bar, 1 µm. (N) *Skeletonema grethae*, strain CCAP1077/3, copula with the ligula (arrow) and the small antiligula (arrowhead). Scale bar, 1 µm.

rimoportula process (RPP), of variable length. In internal view, the RP appears as a slit with two lips oriented radially or obliquely (Fig. 1K). The RP of terminal valves (TRP) is generally located subcentrally, sometimes close to the annulus (Fig. 1B) or up to halfway between the center and the valve margin (Fig. 1K). *Skeletonema costatum* (*sensu stricto*) and *S. grevillei* Sarno et Zingone have a marginal TRP (Zingone et al. 2005). The long external process of the terminal rimoportula (TRPP) widens more or less abruptly toward its distal end (Fig. 1, C and E). In intercalary valves, the RP (intercalary rimoportula, IRP) is located peripherally, near the ring of strutted processes, and bears a short external process (process of the intercalary rimoportula, IRPP) (Fig. 1G), with the exception of *S. subsalsum* and *S. costatum*, where the IRPP is long. In most cases, size and location of the RP allow terminal valves to be distinguished from intercalary valves in broken colonies or loose valves. In addition, the presence of long subcentral RPPs marks the point at which a colony will split into two.

The girdle (Fig. 1L) consists of a variable number of open bands. The first band (valvocopula) (Fig. 1M) is narrow and more silicified than the others (copulae). Each copula has a ligula and a small antiligula (Fig. 1N). A siliceous ridge runs along the whole length of the copula and is generally located in a median position, but it is displaced toward one margin in the copulae closer to the valvocopula. The longitudinal ridge is flanked on both sides by transverse ribs, sometimes branching toward their ends. The ribs are interspaced by either rows of pores (0.02–0.04 μm) or by smooth hyaline areas with very fine perforations (approximately 2 nm).

Markedly different size classes were observed in many species (*S. dohrnii*, *S. grethae*, *S. marinoi*, *S. menzelii*, *S. pseudocostatum*, and *S. tropicum*), particularly in recently established cultures, along with cell enlargement within a single colony. Gametes were never observed, and the larger size classes were probably a result of vegetative enlargement (Gallagher 1983).

Skeletonema dohrnii Sarno et Kooistra, sp. nov. (Fig. 2, A–I)

Cellulae longas catenas formantes. Valvae diameter 4–12 μm longus. In cellula quaque 1–2 chloroplasti. Tubuli externi fultoportularum divisi semper. Tubulorum partes extremae planae, expansae et dentatae. Tubulus quisque iunctus est cum uno aut duobus tubulis valvae sororis. Rimoportula iuxta marginem in valvis intercalaribus et subcentraliter in valvis terminalibus posita est. Tubulus externus rimoportulae brevis in valvis intercalaribus, longus in valvis terminalibus. Teniae costis transversis in ramos divisis et areis hyalinis interpositis, raro seriebus porulorum, praeditae sunt.

Cells forming long chains. Valve diameter 4–12 μm. Each cell contains 1–2 chloroplasts. External processes of the fultoportulae open, with flat and flared tips and jagged distal margins. Each process links to one or two processes of the sibling valve. The rimoportula is located close to the valve face margin in intercalary valves and in a subcentral position in terminal valves. External process of the rimoportula short in intercalary valves, long in terminal valves of the colony. The copulae have transverse, branched ribs. The ribs are interspaced by hyaline areas, rarely by series of pores.

Holotype: A permanent slide of strain SZN-B104 has been deposited at the SZN Museum as no. SZN-B104/1.

Iconotype: Figure 2, A–I.

Material examined: Strains SZN-B104, SZN-B105, and SZN-B191.

Type locality: Gulf of Naples, Italy (South Tyrrhenian Sea, Mediterranean Sea).

Etymology: The species epithet is derived from Anton Dohrn (1840–1909), evolutionist and fervent supporter of Darwinism, who founded the SZN.

Description: Cells 4–12 μm in diameter, forming long colonies (Fig. 2A), often curved or coiled. The valve face is slightly convex, with a prominent network of costae delimiting rectangular areolae, which become pseudoloculate toward the mantle (Fig. 2, B and F). The TFPPs and IFPPs are split and have flat and flared tips and jagged distal margins (Figs. 1, C and D, and 2, C–E). The IFPPs of adjacent cells can be either aligned, with a 1:1 linkage (Fig. 2D), or displaced, with a 1:2 linkage (Fig. 2E). The 1:2 linkage may extend along the whole junction, which appears as a zigzag line (Figs. 1J and 2G). The IFPPs interlock is a plain joint, with no intricate knots or knuckles. The flared edges of the IFPPs seem to overlap with interdigitating edges (Fig. 2, D, E, and G). The TRP is subcentral and has a long tubular process that is sometimes cup shaped at its apex (Fig. 2, B and C). The IRP is located marginally and bears a short, at times flared, external process (Fig. 2D). The copulae have transverse branched ribs, delimiting hyaline interspaces (Fig. 2H). In clone SZN-B104, a pattern of irregularly spaced series of pores is occasionally observed (Fig. 2I).

Note: The species is found in the Gulf of Naples, where it is recorded rarely and with low abundances in winter.

Skeletonema grethae Zingone et Sarno sp. nov. (Fig. 3, A–I)

Cellulae longas catenas formantes. Valvae diameter 2–10.5 μm longus. In quaque cellula 1–2 chloroplasti. Tubuli externi fultoportularum divisi. Partes extremae tubulorum truncatae vel ut ungues. Tubulus quisque iunctus est cum tubulo valvae sororis. Interdum tubulus iunctus est cum duobus tubulis valvae sororis. Rimoportula iuxta marginem in valvis intercalaribus et subcentraliter in valvis terminalibus catenae posita est. Tubulus externus rimoportulae brevis in valvis intercalaribus, longus in valvis terminalibus catenae. Teniae costis transversis et areis hyalinis interpositis praeditae sunt.

Cells forming long chains. Valve diameter 2–10.5 μm. Each cell contains 1–2 chloroplasts. External processes of the fultoportulae open, truncated, or with a claw-like protrusion. Each process connects with one process of the sibling valve. Occasionally, one process joins two

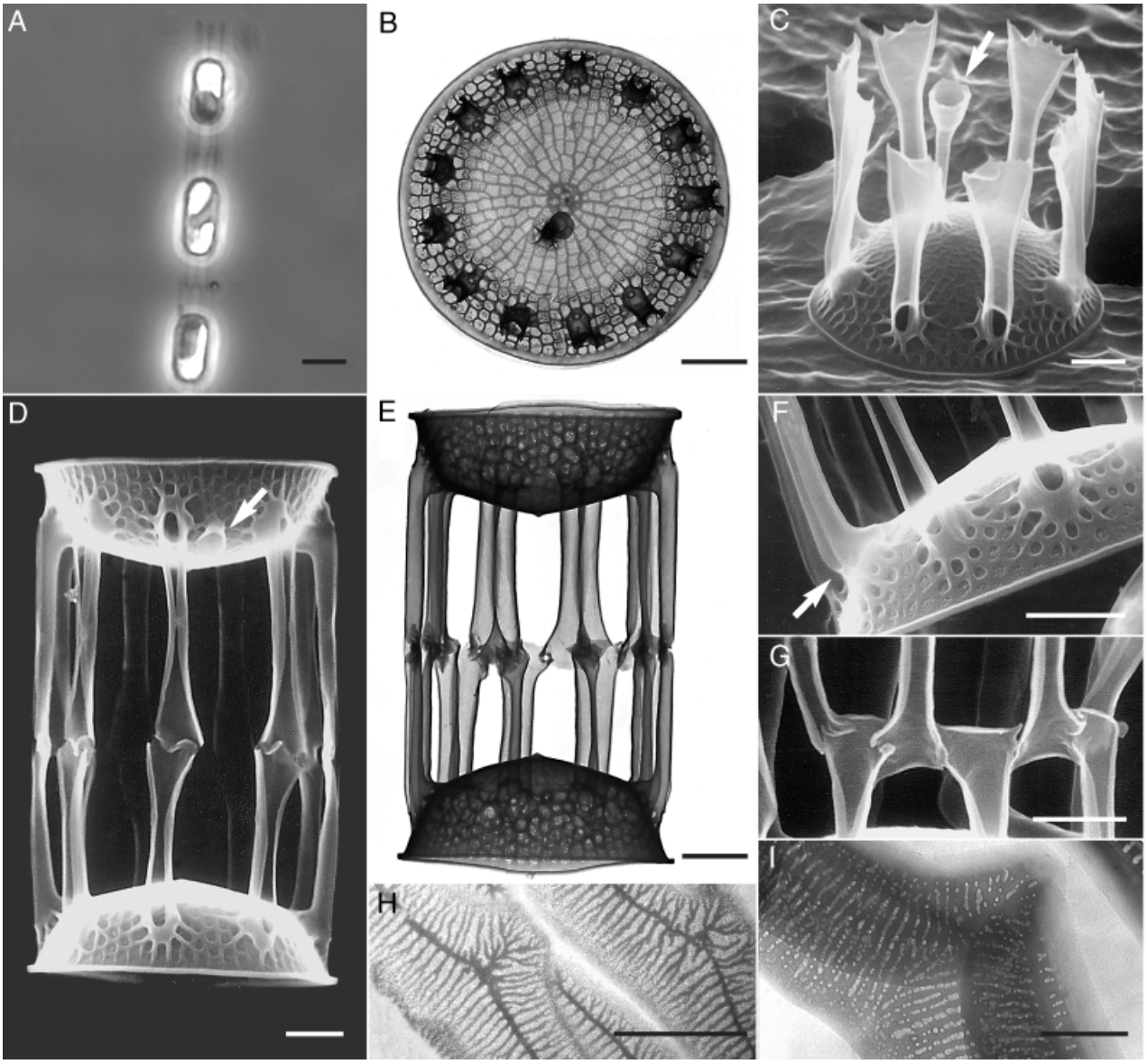

FIG. 2. *Skeletonema dohrnii*. LM: A; SEM: C, D, F, and G; TEM: B, E, H, and I. (A) Strain SZN-B104, colony in girdle view. Scale bar, 10 μm. (B) Strain SZN-B104, terminal valve of a colony in valve view, with the slightly subcentral TRPP. Scale bar, 1 μm. (C) Strain SZN-B104, terminal valve with the long and tubular TRPP (arrow) and the flared tips and jagged margins of TFPPs. Scale bar, 1 μm. (D) Strain SZN-B104, intercalary valves with IFPPs joined in a 1:1 fashion and the marginal IRPP (arrow). Scale bar, 1 μm. (E) Strain SZN-B104, intercalary valves with IFPPs joined in a 1:2 fashion. Scale bar, 1 μm. (F) Strain SZN-B104, detail of terminal valve with pseudoloculate areolae. Note the TFPPs entirely split at their base (arrow). Scale bar, 1 μm. (G) Strain SZN-B105, detail of the 1:2 connections. Scale bar, 1 μm. (H) Strain SZN-B105, cingular bands with ribs delimiting hyaline interspaces. Scale bar, 1 μm. (I) Strain SZN-B104, cingular band with irregular series of pores. Scale bar, 0.5 μm.

processes of the sibling valve. The rimoportula is located close to the valve face margin in intercalary valves and in a subcentral position in terminal valves. External process of the rimoportula short in intercalary valves, long in terminal valves of the colony. Copulae with transverse ribs interspaced by hyaline areas.

Holotype: A permanent slide of strain CCAP 1077/3 has been deposited in the SZN Museum as no. CCAP 1077/3/2.

Iconotype: Figure 3, A–I.

Material examined: Strains CCAP 1077/3, CCMP 780, and SZN-B190.

Type locality: Narragansett Bay, USA (North Atlantic Ocean).

Etymology: The species is dedicated to Prof. Grethe R. Hasle, eminent diatom specialist who conducted the first detailed analysis of *Skeletonema* using the electron microscope.

Synonym: S. costatum sensu Medlin et al. (Medlin et al. 1991).

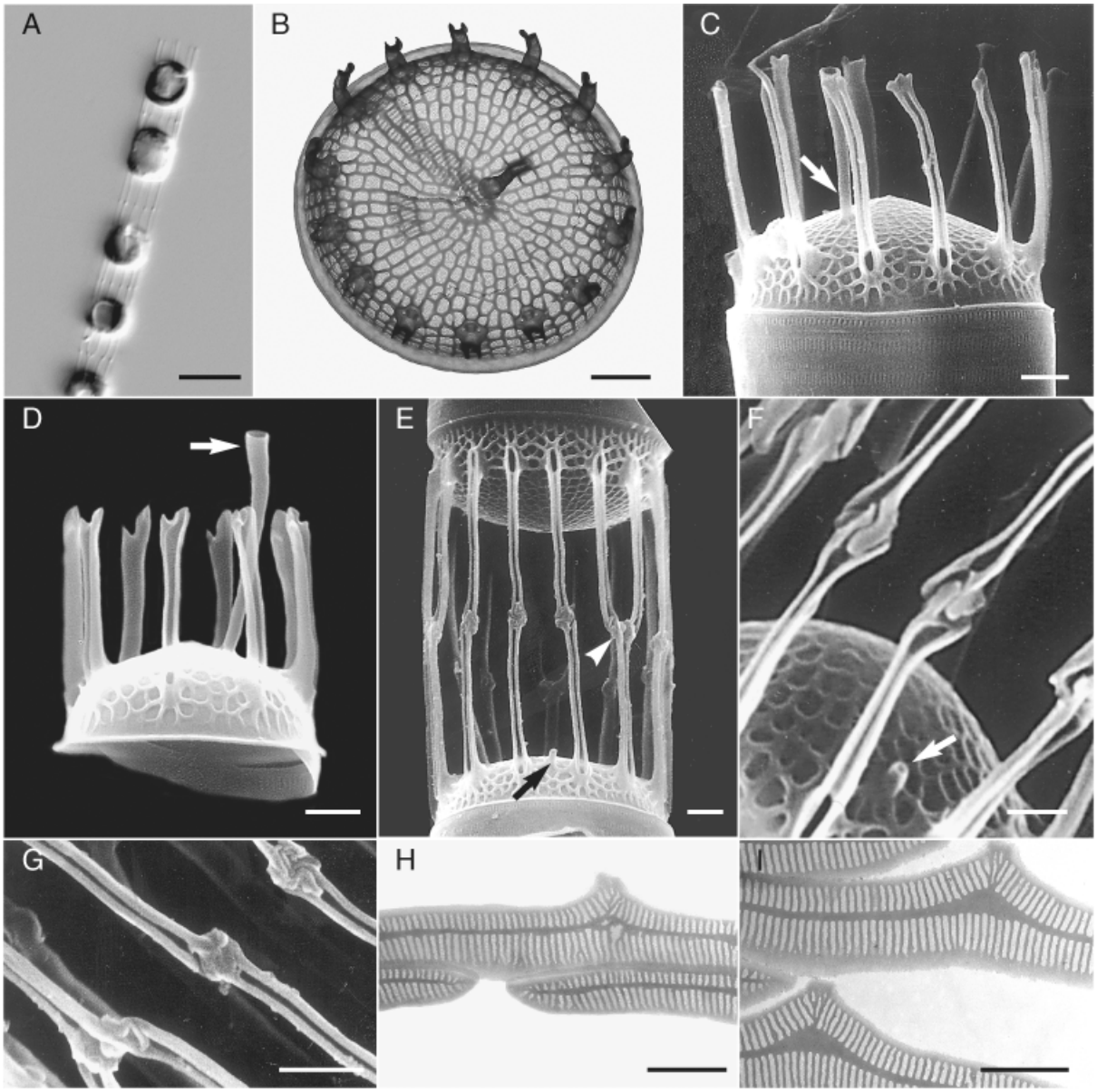

FIG. 3. *Skeletonema grethae*, strain CCAP1077/3, unless otherwise specified. LM: A; SEM: C–G; TEM: B, H, and I. (A) Strain SZN-B190, colony. Scale bar, 20 µm. (B) Terminal valve with the subcentral TRPP. Scale bar, 1 µm. (C) Terminal valve showing TFPPs with truncated distal margins and the TRPP (arrow). Scale bar, 1 µm. (D) Terminal valve with claw-like TFPPs ends and the subcentral TRPP (arrow). Scale bar, 1 µm. (E) Intercalary valves with IFPPs joined in a 1:1 fashion, a single 1:2 junction (arrowhead), and the IRPP (arrow). Scale bar, 1 µm. (F) Detail of IFPP junctions and IRPP (arrow). Scale bar, 0.5 µm. (G) Detail of IFPP junctions. Scale bar, 1 µm. (H) Cingular band with ribs interspaced by hyaline areas. Scale bar, 1 µm. (I) Cingular bands with more silicified central ridge. Scale bar, 1 µm.

Description: Cells 2–10.5 µm in diameter, forming extremely long colonies (up to 111 cells in strain CCAP 1077/3) (Fig. 3A), at times bent or coiled. The valve face is slightly convex. The TFPPs are open and show narrow distal ends that can either be truncated with an irregular margin (Fig. 3C) or have a finger-or claw-like protrusion (Fig. 3D). The IFPPs are also narrow and are generally aligned and joined in a 1:1 fashion with those of the contiguous valves. Occasionally, one IFPP joins two IFPPs of the sibling valve (1:2 junction) (Fig. 3, E–G), but a transverse zigzag line along the junction has never been observed. The interlocking between IFPPs of sibling valves is sometimes a fork joint (Fig. 3F) but can be particularly intricate and tight, like a knot or a knuckle (Fig. 3, E and G). The TRP is subcentral and has a long process with a slightly flared apical opening (Fig. 3, B–D). The IRP is marginal and has a short process (Fig. 3, E and F). In the copulae, the transverse ribs are interspaced by hyaline areas (Fig. 3, H and I).

Skeletonema japonicum Zingone et Sarno, sp. nov. (Fig. 4, A–J)

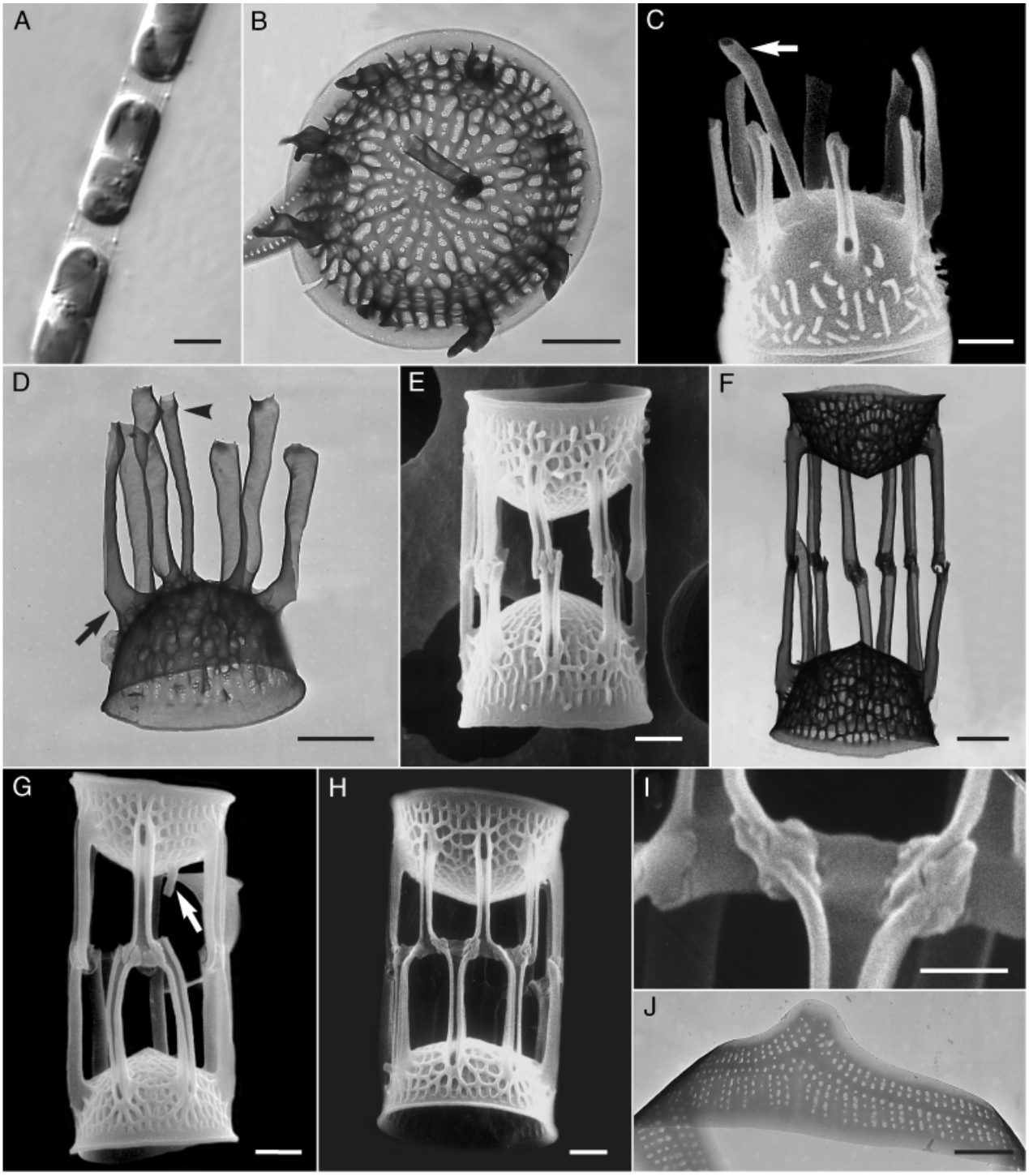

FIG. 4. *Skeletonema japonicum*, strain SZN-B149. LM: A; SEM: C, E, and G–I; TEM: B, D, F, and J. (A) Colony. Scale bar, 5 µm. (B) Terminal valve with the subcentral TRPP. Scale bar, 1 µm. (C) Terminal valve with truncated TFPP ends and the subcentral TRPP (arrow). Scale bar, 1 µm. (D) Terminal valve, showing TFPPs with a tubular basal part (arrow) and the TRPP (arrowhead). Scale bar, 1 µm. (E) Intercalary valves with slightly displaced IFPPs and fork-shaped joints. Scale bar, 1 µm. (F) Intercalary valves with fork-shaped IFPP joints. Scale bar, 1 µm. (G) Intercalary valves with a single 1:2 IFPP junction and IRPP (arrow). Scale bar, 1 µm. (H) Intercalary valves showing 1:2 junctions. Scale bar, 1 µm. (I) Detail of 1:2 junction. Scale bar, 0.5 µm. (J) Cingular band with uniseriate rows of pores. Scale bar, 0.5 µm.

Cellulae longas catenas formantes. Valvae diameter 2–10 µm longus. In cellula quaque 1–2 aut raro 3–4 chloroplasti. Tubuli externi fultoportularum divisi in valvis intercalaribus, clausi ad basim in valvis terminalibus catenae. Partes extremae tubulorum truncatae sunt. Quisque tubulus iunctus uno aut duobus tubulis valvae sororis. Rimoportula

iuxta marginem in valvis intercalaribus sed subcentraliter in valvis terminalibus posita est. Tubulus externus rimoportulae curtus in valvis intercalaribus, longus in valvis terminalibus. Teniae costis transversis et seriebus porulorum interpositis praeditae sunt.

Cells forming long chains. Valve diameter 2–10 μm. Each cell contains 1–2, rarely 3–4 chloroplasts. External processes of the fultoportulae are open in intercalary valves, closed at their base in terminal valves of the colony. Distal ends of the processes truncated. Each process connects with one or two processes of the sibling valve. The rimoportula is located close to the valve face margin in intercalary valves and subcentrally in terminal valves. External process of the rimoportula short in intercalary valves, long in terminal valves of the colony. Copulae with transverse ribs interspaced by rows of pores.

Holotype: A permanent slide of strain SZN-B149 has been deposited in the SZN Museum as no. SZN-B149/3.

Iconotype: Figure 4, A–J.

Material examined: Strain SZN-B149.

Type locality: Hiroshima Bay, Seto Inland Sea, Japan (North Pacific Ocean).

Etymology: The epithet *japonicum* (= Japanese) refers to the type locality of the species.

Description: Cells 2–10 μm in diameter, forming long colonies. Each cell has one to two, rarely three to four, chloroplasts (Fig. 4A). The valve face is slightly convex, with a conspicuous network of costae delimiting radial rows of areolae of irregular shape (Fig. 4B). In some specimens, spines or ridges are scattered on the surface or a thick siliceous layer covers the valve, partially or completely occluding the areolae (Fig. 4, C and D). The basal part of the TFPPs is tubular and oblique to the cell axis, forming an angle with the rest of the process, which is open along its length and parallel to the cell axis (Fig. 4, C and D). The distal end of the TFPPs is narrow and generally truncated, with a slightly jagged rarely claw-like margin (Fig. 4, C and D). The IFPPs are open and are connected in a 1:1 or 1:2 mode. In the 1:1 junction type, the adjoining IFPPs are slightly displaced, and their narrow distal ends interdigitate in a fork joint (Fig. 4, E and F). In the 1:2 junction type, the IFPPs are displaced and flared at their distal ends, each tip forming knot-like junctions with the flared ends of two opposite IFPPs (Figs. 1I and 4, G–I). The TRP has long and tubular process emerging close to the valve center (Fig. 4, B–D). The IRP has a short external tube and is located near the valve margin (Fig. 4G). In the copulae, the transverse ribs are interspaced by rows of pores (Fig. 4J).

Skeletonema marinoi Sarno et Zingone, sp. nov. (Fig. 5, A–H)

Cellulae longas catenas formantes. Valvae diameter 2–12 μm longus. In cellula quaque 1–2 chloroplasti. Tubuli externi fultoportularum divisi. Partes extremae tubulorum planae, expansae et dentatae. Tubulus quisque iunctus uno aut duobus tubulis valvae sororis. Rimoportula iuxta marginem in valvis intercalaribus et subcentraliter in valvis terminalibus posita est. Tubulus externus rimoportulae brevis in valvis intercalaribus, longus in valvis terminalibus. Teniae costis transversis et seriebus porulorum interpositis praeditae sunt.

Cells forming long chains. Valve diameter 2–12 μm. Each cell contains 1–2 chloroplasts. External processes of the fultoportulae open, with flat and flared tips and jagged distal margins. Each process connects with one or two processes of the sibling valve. The rimoportula is close to the valve face margin in intercalary valves and subcentral in terminal valves. External process of the rimoportula short in intercalary valves, long in terminal valves of the colony. Copulae with transverse ribs interspaced by rows of pores.

Holotype: A permanent slide of strains SZN-B120 and SZN-B146 has been deposited in the SZN Museum as nos. SZN-B120/4 and SZN-B146/5.

Iconotype: Figure 5, A–H.

Material examined: Strains SZN-B118, SZN-B119, SZN-B120, SZN-B121, SZN-B146, SZN-B147, SZN-B189, and CCMP 1009.

Type locality: North Adriatic Sea, Mediterranean Sea.

Etymology: The species is dedicated to Donato Marino (1947–2002), who introduced phytoplankton studies at SZN and taught diatom taxonomy to two of the authors (A. Z. and D. S.).

Description: Cells 2–12 μm in diameter, forming long (Figs. 1A and 5A), often curved or coiled colonies. Each cell contains one or two chloroplasts. The valve face is slightly convex; the mantle is vertical (Fig. 5F). The FPPs are open along their entire length (Fig. 5, C–F). Their distal end is flattened and flared, with a dentate margin (Fig. 5, C ands D). The IFPPs of sibling valves can either be aligned, with a 1:1 linkage (Fig. 5E), or displaced, with a 1:2 linkage and a zigzag connection line (Fig. 5, F and G). The interlocking between IFPPs is in all cases a plain joint, with no intricate knots or knuckles. The flared tips of the IFPPs overlap with edges that interdigitate with one another (Fig. 5, E–G). The TRP is located close to the central annulus or midway between the center and the margin of the valve and has a long tubular process with a slightly flared or trumpet-or cup-shaped apex (Fig. 5, B–D). The IRP is short and at the edge of the valve face (Fig. 5E). The copulae show the typical central ridge, which is flanked on both sides by transverse ribs interspaced by rows of pores (Figs. 1L and 5H).

Notes: The species is common and abundant in the Adriatic Sea, where it blooms in winter. The other strains examined were from Hong Kong and from the east coast of the United States.

Skeletonema menzelii Guillard, Carpenter et Reimann (Fig. 6, A–G)

Material examined: Strains SZN-B82 and SZN-B83.

Description: Cells 2–7 μm in diameter (up to 10 μm in natural samples), lenticular to cylindrical, depending on cingulum development, solitary or in pairs

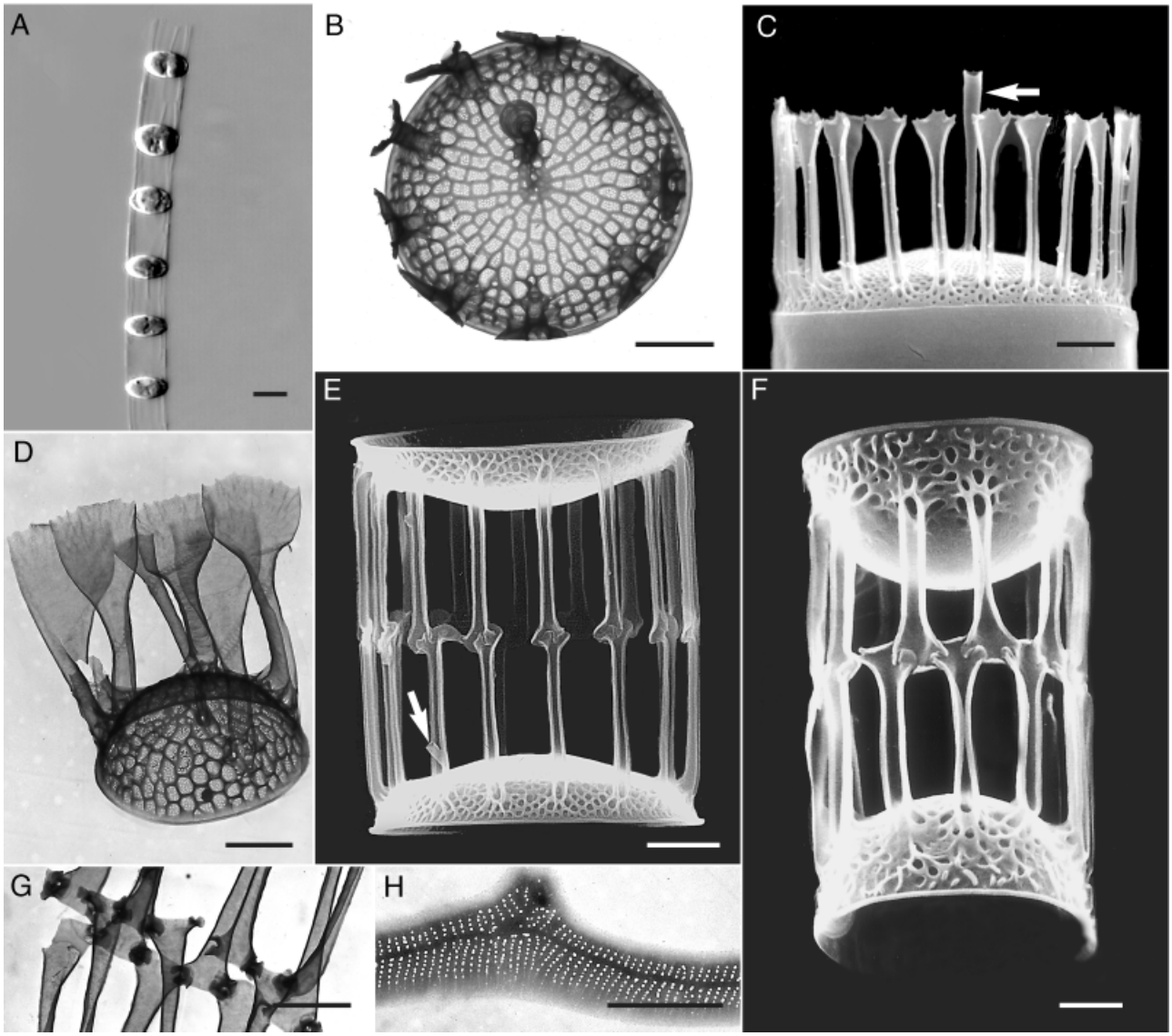

FIG. 5. *Skeletonema marinoi*. LM: A; SEM: C, E, and F; TEM: B, D, G, and H. (A) Strain CCMP1009, colony. Scale bar, 5 μm. (B) Strain SZN-B119, terminal valve with the subcentral TRPP. Scale bar, 1 μm. (C) Strain SZN-B121, terminal valve showing flared ends of TFPPs with dentate margins and the TRPP (arrow). Scale bar, 2 μm. (D) Strain SZN-B119, terminal valve of a colony. Scale bar, 1 μm. (E) Strain SZN-B121, intercalary valves with IFPPs connected with 1:1 plain joints and the IRPP (arrow). Scale bar, 2 μm. (F) Strain SZN-B120, intercalary valves with 1:2 IFPP junctions. Scale bar, 1 μm. (G) Strain SZN-B118, detail of the zigzag connection. Scale bar, 1 μm. (H). Strain SZN-B120, cingular band with uniseriate rows of pores. Scale bar, 1 μm.

(Fig. 6A). Colonies are not observed. The frustule is weakly silicified. The valves are markedly convex with an inconspicuous mantle consisting of a low hyaline border (Fig. 6, B, C, and E). Delicate ribs, branching dichotomously, run radially on the valve face starting from an irregularly structured central area (Fig. 6, B and E). Because of the absence of tangential ribs, no areolae are formed. Barely visible perforations are scattered on the valve (Fig. 6C). Ribs have at times small external spines (Fig. 6, D and E). The FPs have open, narrow, and relatively long processes (Fig. 6, D and E, and Table 2), with two satellite pores in their basal part (Fig. 6C) and two or three marginal spines toward their distal end (Fig. 6, D and E). The RP is situated on the border of the central area; it has a long tubular process gradually expanding distally (Fig. 6, B and E). Neither marginal RPs nor stable connections between FPPs of contiguous valves have been observed. Both these characters are typical of intercalary valves in other species; therefore, their absence in *S. menzelii* suggests that cell pairs are dividing cells. The copulae are characterized by a weakly silicified median ridge and thin transverse ribs at times branching at their ends (Fig. 6, F and G). The ribs are interspaced by hyaline areas.

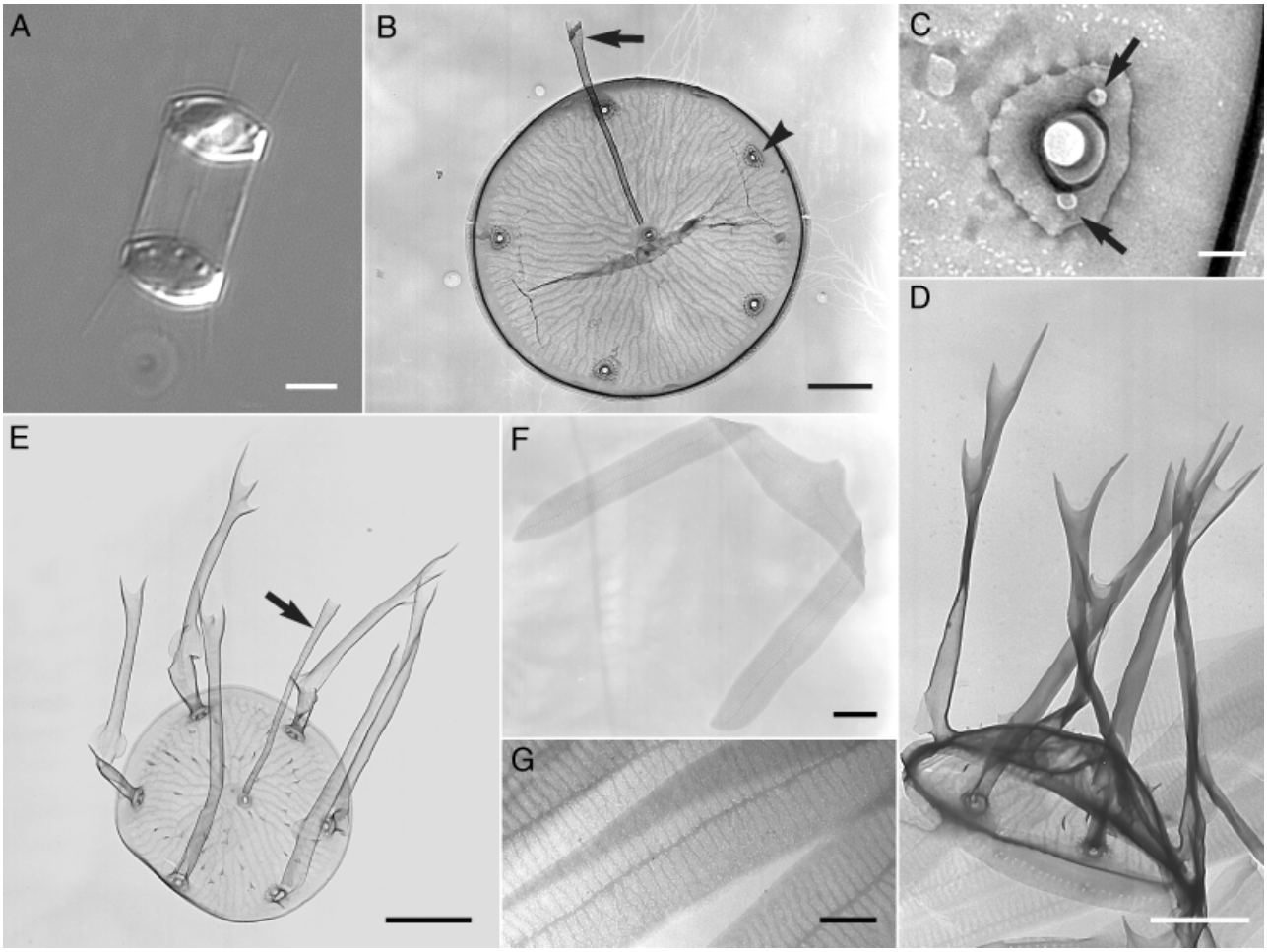

FIG. 6. *Skeletonema menzelii*. LM: A; TEM: B–G. (A) Natural sample, Gulf of Naples (2 October 2001), cells in couplet. Scale bar, 2 μm. (B) Strain SZN-B82, valve with subcentral RPP (arrow) and the FPs (arrowhead). Scale bar, 1 μm. (C) Strain SZN-B82, detail of valve showing a FP with two satellite pores (arrows). Scale bar, 0.1 μm. (D) Strain SZN-B83, valve in girdle view with FPPs showing two or three spines. Scale bar, 1 μm. (E) Strain SZN-B83, valve with subcentral RPP (arrow) and small spines on the valve face. Scale bar, 1 μm. (F) Strain SZN-B83, cingular band. Scale bar, 1 μm. (G) Strain SZN-B83, cingular bands with thin transverse ribs. Scale bar, 0.5 μm.

Notes: The species is commonly found in the Gulf of Naples in autumn and winter, with concentrations up to 2.8×10^4 cells $\cdot$ mL^{-1}. The morphology of the strains from the Western Sargasso Sea and the Gulf of Maine (North Atlantic Ocean) (Guillard et al. 1974) was not examined in this study.

Skeletonema pseudocostatum Medlin emend. Zingone et Sarno (Fig. 7, A–I)

Cells solitary or in chains. Valve diameter 2–9 μm. Each cell contains one to two chloroplasts. External processes of the FP open in intercalary valves, closed at their bases in terminal valves of the colony, distal ends truncated or claw-like. Each process connects with one process of the sibling valve. Occasionally, one process joins two processes of the sibling valve. The RP is marginal in intercalary valves and subcentral in terminal valves. External process of the RP short in intercalary valves, long in terminal valves of the colony. Copulae with transverse ribs interspaced by hyaline areas.

Material examined: Strains SZN-B77, SZN-B78, SZN-B79, SZN-B80, SZN-B81, SZN-B139, SZN-B140, and CCAP1077/7.

Description: Cells 2–9 μm in diameter, solitary or forming relatively short chains (maximum, 34 cells) in culture and in natural samples (Fig. 7A). Slightly convex valves. Rectangular to triangular areolae become pseudoloculate near the mantle (Figs. 1B and 7, B and C). The basal part of the TFPPs is tubular and oblique to the cell axis, forming an angle with the rest of the process, which is open along its length and parallel to the pervalvar axis of the cell. The TFPPs have a narrow tip which can be truncated, spiny, or claw-like (Fig. 7, C and D). The IFPPs are narrow, completely open, and connect to those of adjacent cells by a fork joint or by a knot-or knuckle-like connection (Fig. 7, E–H). The connection is most often of the 1:1 type, but occasionally one IFPP is connected with two opposite IFPPs (Fig. 7G). The TRP is subcentral and has a long process (Fig. 7, B and C). The IRP is marginal and has

TABLE 2. Morphometric characters in *Skeletonema* species.

		S. dorhnii	*S. grethae*	*S. japonicum*	*S. marinoi*	*S. menzelii*	*S. pseudocostatum*	*S. subsalsum*	*S. tropicum*
Cell diameter (μm)	Min–max	4–12	2–10.5	2–10	2–12	2–7	2–9	4–8	5.3–10
	Mean ± SD	6.3 ± 2.6	4.1 ± 1.6	5.3 ± 2.7	4.3 ± 1.9	4.2 ± 1.0	4.7 ± 1.4	5.4 ± 1.0	8.0 ± 1.5
	n	133	56	59	300	30	455	37	42
Cells per colony	Min–max	3–94	9–111	3–64	2–45	—	1–34	7–60	6–93
	Mean ± SD	17.3 ± 12.8	38.9 ± 16.0	15.6 ± 12.0	16.2 ± 10.9	—	6.4 ± 5.3	24.6 ± 15.9	34.9 ± 25.2
	n	92	39	55	125	—	393	30	33
Areolae in 10 μm	Min–max	38–47	33–48	31–40	33–58	—	30–44	41–45	26–33
	Mean ± SD	42.1 ± 3.4	41.7 ± 6.4	35.8 ± 3.1	40.9 ± 5.9	—	35.9 ± 4.8	43 ± 3.8	32 ± 3.4
	n	7	4	13	24	—	11	2	4
FPPs per cell	Min–max	8–13	14–19	6–8	9–11	6–10	7–18	12–17	11–13
	Mean ± SD	10 ± 1.8	16.5 ± 3.5	7.4 ± 0.9	10 ± 1	7.3 ± 2.3	11 ± 3.9	14 ± 2.3	11.5 ± 2.1
	n	6	3	10	5	3	16	5	2
Distance between FPPs (μm)	Min–max	0.6–0.8	0.2–1.0	0.9–1.9	0.5–1.5	1.3–2.1	0.4–1.3	0.5–1.0	0.6–1.3
	Mean ± SD	0.7 ± 0.3	0.7 ± 0.2	1.1 ± 0.3	0.9 ± 0.2	1.6 ± 0.4	0.7 ± 0.2	0.8 ± 0.2	0.9 ± 0.2
	n	9	19	9	26	4	31	5	7
IFPP length (μm)	Min–max	2.8–4	2.0–4.5	1.5–3.6	1.1–4.2	—	5.6–1.0	0.6–2.7	1.2–4.1
	Mean ± SD	2.9 ± 1.3	3.5 ± 0.7	2.7 ± 0.7	2.6 ± 0.8	—	2.6 ± 1.2	1.8 ± 0.6	2.6 ± 0.8
	n	12	18	11	38	—	25	14	10
IFPP width (μm)	Min–max	0.2–0.4	0.1–0.3	0.2–0.5	0.1–0.5	—	0.1–0.4	0.3–0.5	0.1–0.5
	Mean ± SD	0.3 ± 0.5	0.2 ± 0.1	0.4 ± 0.1	0.3 ± 0.1	—	0.2 ± 0.1	0.4 ± 0.1	0.3 ± 0.1
	n	10	22	11	37	—	50	9	10
TFPP length (μm)	Min–max	2.4–5.1	1.4–4.7	1.4–3.1	1.4–1.5	3.4–6.3	1.1–4.1	2.6–2.7	2.1–3.5
	Mean ± SD	3.6 ± 1.0	3.4 ± 1.0	2.2 ± 0.5	2.9 ± 1.3	4.8 ± 0.2	2.5 ± 1.1	2.6 ± 0.1	2.8 ± 0.5
	n	6	8	11	20	2	25	2	7
TFPP tubular part length (μm)	Min–max	0.0–0.3	0.0–0.3	0.0–0.5	0.0–0.3	0.0	0.3–0.8	0.0	0.0–0.7
	Mean ± SD	0.1 ± 0.1	0.1 ± 0.1	0.4 ± 0.1	0.1 ± 0.1	0.0 ± 0.0	0.5 ± 0.1	0.0 ± 0.0	0.4 ± 0.3
	n	7	6	13	21	3	20	2	8
TFPP basal part width (μm)	Min–max	0.3–0.5	0.2–0.4	0.1–0.4	0.1–0.5	0.3–0.5	0.1–0.4	0.4–0.5	0.2–0.6
	Mean ± SD	0.3 ± 0.1	0.3 ± 0.1	0.3 ± 0.1	0.3 ± 0.1	0.4 ± 0.1	0.3 ± 0.1	0.4 ± 0.1	0.4 ± 0.1
	n	6	6	12	17	5	18	2	6
TFPP distal part width (μm)	Min–max	0.6–1.0	0.2–0.5	0.2–0.7	0.4–1.3	0.3–0.5	0.2–0.4	0.5	0.4–1.0
	Mean ± SD	0.8 ± 0.1	0.4 ± 0.1	0.4 ± 0.1	0.8 ± 0.3	0.4 ± 0.1	0.3 ± 0.1	—	0.5 ± 0.2
	n	8	6	12	31	4	18	1	7
IRPP length (μm)	Min–max	0.2	0.3	0.3–0.7	0.4–0.6	—	0.2–0.6	1.2–3.4	0.7–1.0
	Mean ± SD	0.2 ± 0.0	0.3 ± 0.0	0.4 ± 0.2	0.5 ± 0.1	—	0.4 ± 0.1	2.4 ± 0.9	0.8 ± 0.1
	n	3	2	4	2	—	6	4	3
TRPP length (μm)	Min–max	2.4	1.8–3.6	2.1–3.8	1.4–5.8	2.7–5.4	0.6–2.9	1.8–2.1	2.8–5.3
	Mean ± SD	—	2.9 ± 0.9	2.6 ± 0.6	2.9 ± 1.4	4.0 ± 1.9	1.5 ± 0.8	1.9 ± 0.2	3.8 ± 1.3
	n	1	4	11	9	3	11	2	3
Cingular band ribs in 1 μm	Min–max	14	11–13	11–13	13–15	14–16	14–16	12–13	12–14
	Mean ± SD	—	12 ± 0.6	12 ± 0.5	14 ± 0.7	14 ± 1	15 ± 0.9	12 ± 0.4	13 ± 0.8
	n	1	5	7	9	3	10	3	4

All information is from culture material.

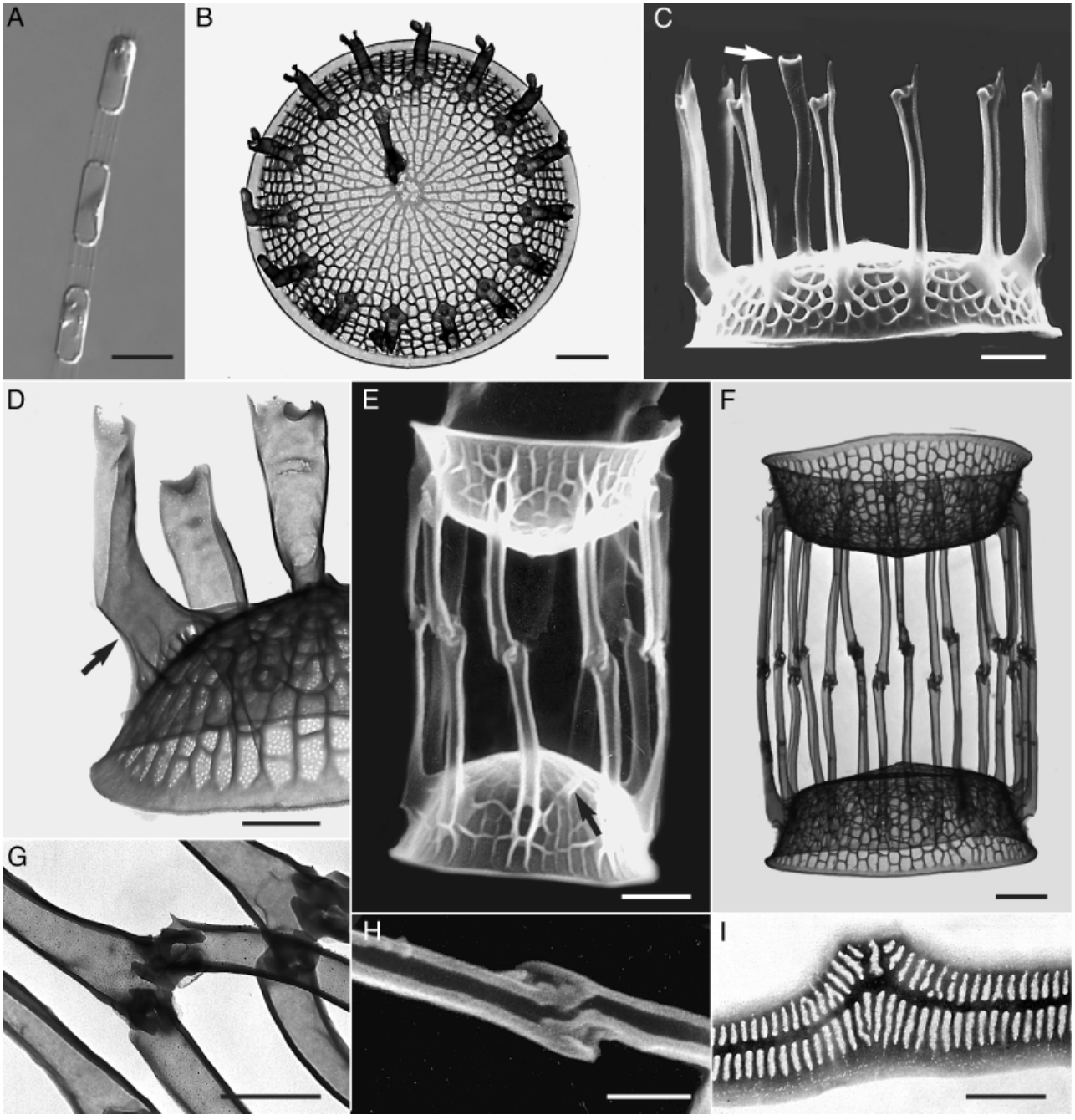

FIG. 7. *Skeletonema pseudocostatum*. LM: A; SEM: C, E, and H; TEM: B, D, F, G, and I. (A) Natural sample, Gulf of Naples (31 July 2001), colony. Scale bar, 10 μm. (B) Strain SZN-B77, terminal valve with subcentral TRPP. Scale bar, 1 μm. (C) Strain SZN-B77, terminal valve, with TFPPs showing spiny ends and TRPP (arrow). Scale bar, 1 μm. (D) Strain CCAP1077/7, detail of a terminal valve. Note the tubular part at the base of TFPP (arrow). Scale bar, 0.5 μm. (E) Strain CCAP1077/7, intercalary valves with 1:1 IFPP junctions and IRPP (arrow). Scale bar, 1 μm. (F) Strain SZN-B77, intercalary valves. Scale bar, 1 μm. (G) Strain SZN-B77, detail of two separate 1:2 junctions. Scale bar, 0.5 μm. (H) Strain SZN-B80, detail of a 1:1 junction. Scale bar, 0.5 μm. (I) Strain CCAP1077/7, cingular bands with transverse ribs interspaced by hyaline areas. Scale bar, 0.5 μm.

a short process (Fig. 7E). In the copulae, transverse ribs are interspaced by hyaline areas.

Notes: This species is often found in its solitary form as the most abundant *Skeletonema* in the Gulf of Naples, where it attains maximum concentrations in May and June (up to 8.6×10^4 cells $\cdot$ mL^{-1}). The other strains examined were from south eastern Mediterranean waters off Alexandria (Egypt) and from south Pacific Ocean (Australia).

Skeletonema subsalsum (Cleve) Bethge (Fig. 8, A–H)

Description: Cells 4–8 μm in diameter, forming colonies that have a very variable intercellular distance

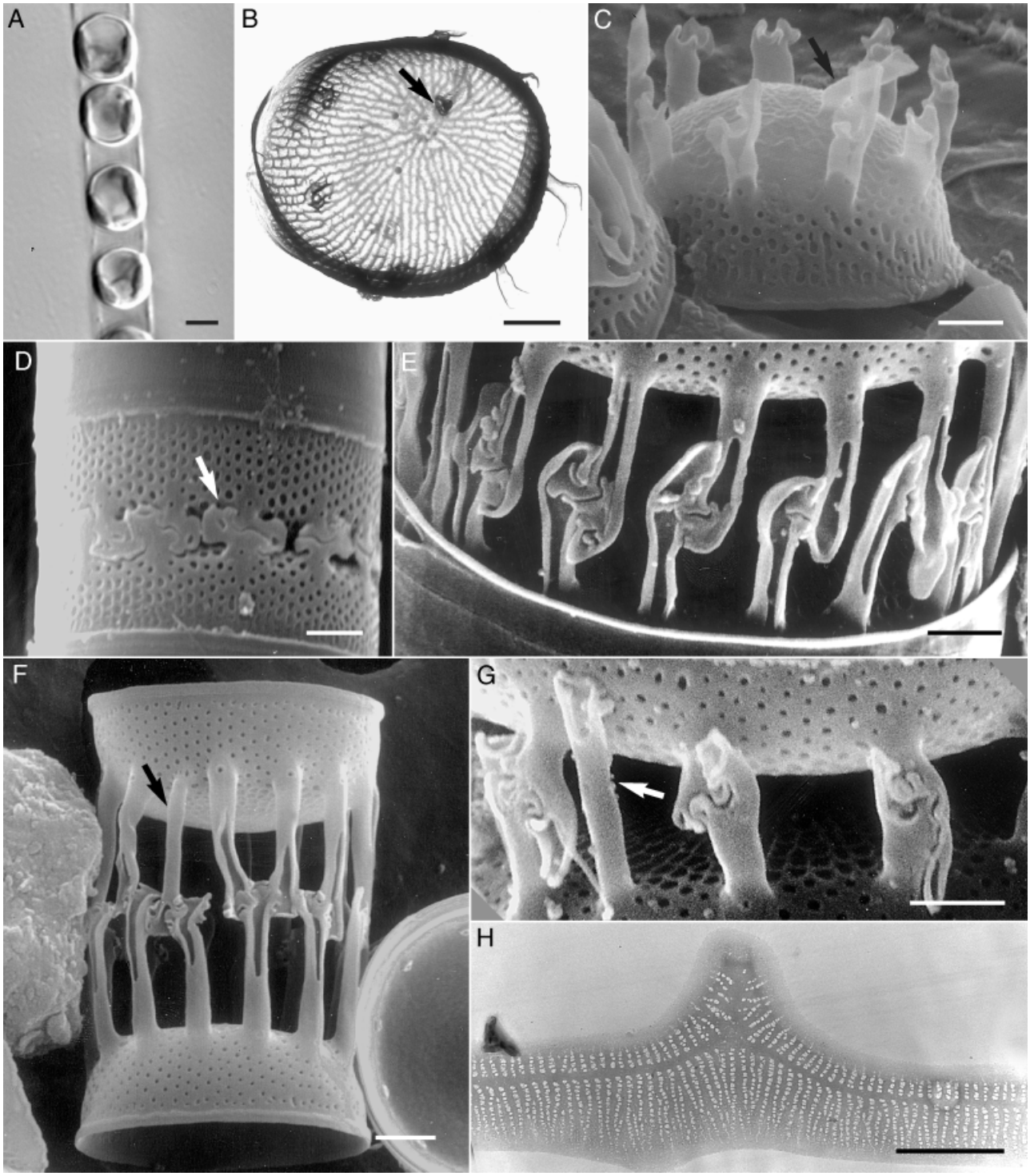

FIG. 8. *Skeletonema subsalsum*, strain CCAP1077/8. LM: A; SEM: C–G; TEM: B and H. (A) Colony. Scale bar, 2 µm. (B) Terminal valve with the subcentral TRP (arrow). Scale bar, 1 µm. (C) Terminal valve with hook-shaped TFPPs ends and TRPP (arrow). Scale bar, 1 µm. (D) Intercalary valves with short IFPPs (arrow). Scale bar, 1 µm. (E) Intercalary valves with 1:1 IFPP junctions. Scale bar, 1 µm. (F) Intercalary valves with 1:2 IFPP junctions; note the long IRPP (arrow) connected with two opposite IFPPs. Scale bar, 1 µm. (G) Detail of sibling valves, with IRPP (arrow) leaning against the contiguous valve. (H) Cingular band with rows of pores. Scale bar, 0.5 µm.

(Fig. 8, A and D–G). The valve face appears rather flat in close-fitting cells (Fig. 8D) and convex and rounded in more distant cells (Fig. 8A). The areolae are mostly rectangular and radially arranged on the valve face (Fig. 8B); on the mantle, the rims of the costae are more heavily silicified and the areolae are

pseudoloculate with an external pore (Fig. 8, C–G). Terminal valves were rarely observed in the colonies of the cultured strain, and they were not clearly illustrated in previous studies. The TFPPs appear as partially closed tubes with an external hole at their base and hook-shaped distal ends (Fig. 8, B and C). The IFPPs vary greatly in length and shape, ranging from very short and apparently closed tubes to longer, open, or partially closed tubes (Fig. 8, D–G). Closed IFPPs usually have an external hole at their base and a longitudinal suture distal to the hole (Fig. 8, D–G). The distal end of the IFPPs is irregularly expanded, with an undulate margin interlocking tightly with that of the sibling IFPPs (Fig. 8, D–G) in a 1:1 or 1:2 fashion (Fig. 8, E and F). The TRP has a long process and is located near the center of the valve (Figs. 1K and 8, B and C). The IRP is located at the rim of the valve face and bears a variably long process with a tea-pot spout-like distal end (Fig. 8G). Sometimes the IRPP is longer than the IFPPs and reaches the valve mantle of the proximate cell. In other cases it is as long as the IFPPs, when it replaces an IFPP and connects to one or to two opposite IFPPs (Fig. 8F). In the copulae, the transverse ribs are interspaced by rows of pores (Fig. 8H).

Material examined: Strain CCAP 1077/8.

Notes: The only strain examined originates from Lough Erne (Ireland), but the species was originally described from the Stockholm Archipelago (Sweden).

Skeletonema tropicum Cleve (Fig. 9, A–H)

Strongly silicified cells, joined in colonies, generally containing 5–10 chloroplasts (Fig. 9A). Smaller cells may have fewer chloroplasts (at least one to two), whereas 30 chloroplasts were seen in a large specimen in a natural sample from the Gulf of Naples. In cultured specimens, cell diameter ranged between 5.3 and 10 μm, but cells of up to 17.5 μm in diameter were observed in natural samples from the Gulf of Naples. The valves are convex with a vertical mantle. On the valve surface, well-developed costae delimit round or oval areolae (Fig. 9B). Pseudoloculi are better developed than in other species. FPPs are open (Fig. 9, C–F), but at times the edges of the longitudinal splits in IFPPs stick together, leaving an elongated opening at the base of the tube (Fig. 9E). The tips of the TFPPs are truncated (Fig. 9D) or, more often, show a stout spine or a claw-like projection (Figs. 1E and 9C). The IFPPs connect tightly to those of the next cell with a knuckle-like junction (Fig. 9, E–G). The junction is generally of the 1:1 type (Fig. 9, E and F), but occasionally single 1:2 junctions are seen (Fig. 1, G and H). In the strains from the Gulf of Naples, contiguous 1:2 connections detected as a zigzag line have been observed along half a cell circumference (Fig. 9G). The TRP has a long, external, trumpet-shaped process, located near the central annulus or midway between the annulus and the valve margin (Fig. 9, C and D). The IRPP is shorter and situated slightly inside the ring of marginal intercalary FPs (Fig. 9E). In the copulae, the transverse ribs are well silicified and interspaced by rows of pores (Fig. 9H).

Material examined: SZN-B141, SZN-B142, SZN-B143, SZN-B144, SZN-B145, and CCMP 788.

Notes: This species is considered tropical and subtropical, with a distribution not beyond 30° North of the equator, in the western Atlantic Ocean (Hulburt and Guillard 1968). Strains examined were isolated from the Gulf of Mexico and from the Gulf of Naples, where it is recorded in September and October at concentrations up to 2.6×10^2 cells $\cdot$ mL^{-1}.

Sequence data. The 24 nuclear-encoded SSU rDNA sequences of *Skeletonema* strains aligned readily by eye, and only a few gaps needed to be introduced. The alignment contained 1805 positions, of which 61 were parsimony informative. Eight distinct genotypic groups were recognizable, differing in at least five positions. Sequences within a group were identical or, in a few cases, differed only in one or two positions. The SSU sequences of CCAP1077/3, CCAP1077/7, CCAP1077/8, and CCMP1009 were obtained at SZN and compared with those available in GenBank. We only observed differences in two base pairs in the case of CCAP1077/3 and in one base pair in the case of CCAP1077/8; both sequences were retained in the further analyses. SSU sequences of *S. tropicum* and *S. japonicum* failed to amplify.

The SSU sequences were aligned subsequently with ones from other Thalassiosiraceae as well as from *Ditylum brightwellii* (West) Grunow in Van Heurck, *Lithodesmium undulatum* Ehrenberg, *Helicotheca tamesis* (Shrubsole) Ricard, and *Bellerochea malleus* (Brightwell) van Heurck, all from GenBank (Table 1). Nineteen extra gaps were needed, but the original alignment among the *Skeletonema* sequences was retained with the addition of the outgroups. The obtained align ment contained 297 parsimony informative sites. Both the hLRTs and the AIC selected a transitional model ($A \leftrightarrow C = G \leftrightarrow T = 1$, $A \leftrightarrow T = C \leftrightarrow G = 1.7026$, $A \leftrightarrow G = 3.3875$, and $C \leftrightarrow T = 4.8617$) with unequal base composition ($A = 0.2677$, $C = 0.1937$, $G = 0.2527$, $T = 0.2859$), a gamma distribution shape parameter of 0.7448, and a proportion of invariable sites of 0.5389 (TIM + I + G). All ML analyses of the SSU data set were constrained with these settings.

An ML analysis with all sequences (except identical ones) resulted in a single ML tree (Fig. 10). If the four non-thalassiosiracean taxa were chosen as outgroups, *Skeletonema* grouped in a compact clade within a grade of *Thalassiosira*. *Porosira pseudodenticulata* (Hustedt) Jousé and *Lauderia annulata* Cleve formed a clade with conspicuously long end branches. The tree revealed four lineages within *Skeletonema*. In the first, sequences of *S. grethae* were recovered in a clade with *S. pseudocostatum* as sister clade. The second lineage was sister to lineage 1 and included all four sequences of *S. menzelii*. Two sequences of Mediterranean *S. menzelii* strains were virtually identical but differed markedly from those of CCMP787 and CCMP790. In the third lineage, identical sequences of *S. dohrnii* formed a sister clade to one with identical sequences of *S. marinoi*. The fourth lineage only contained

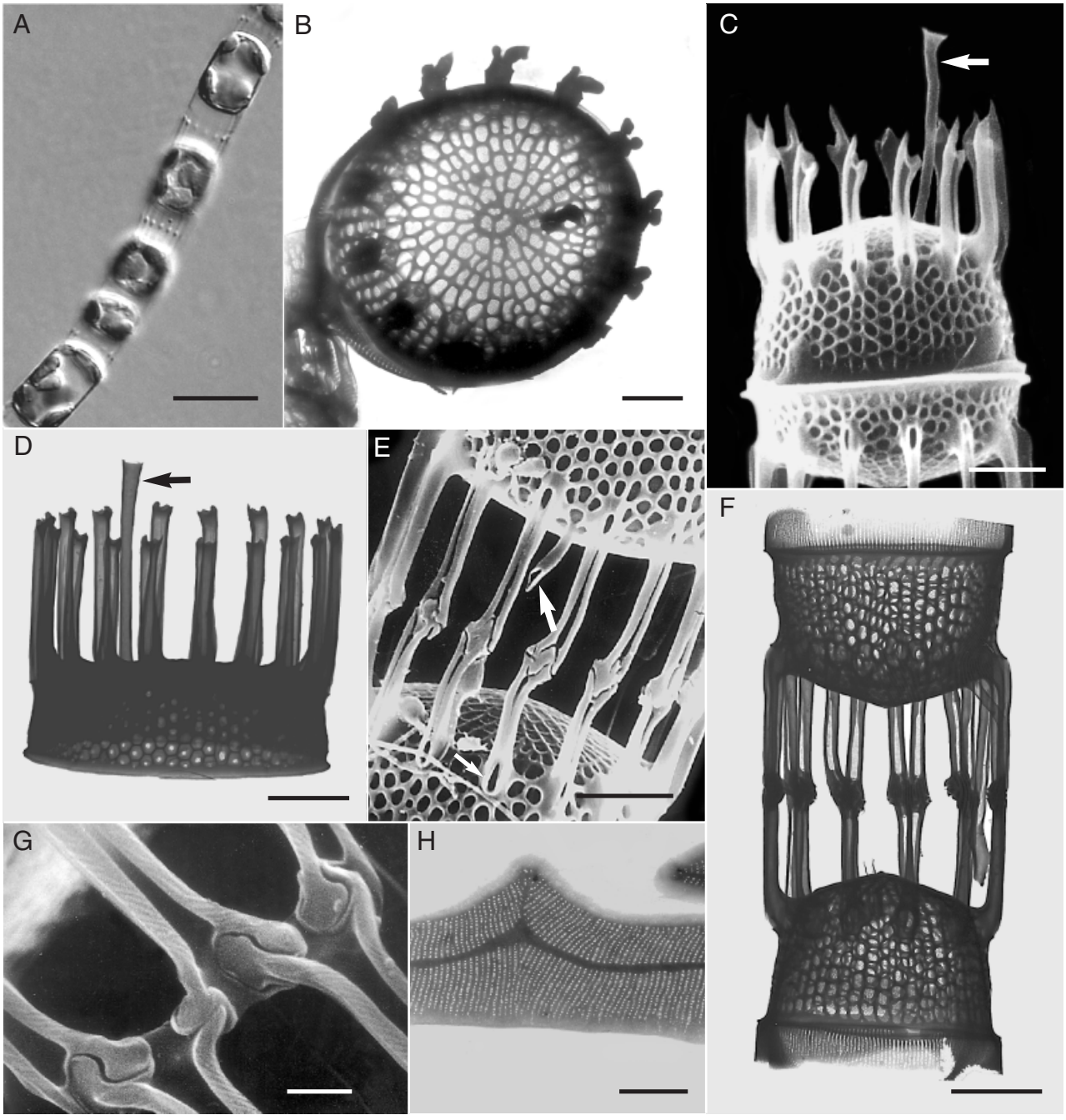

FIG. 9. *Skeletonema tropicum*. LM: A, SEM: C, E, and G; TEM: B, D, F, and H. (A) Strain SZN-B141, colony with numerous chloroplasts in each cell. Scale bar, 10 µm. (B) Strain CCMP788, terminal valve with the subcentral TRPP. Scale bar, 2 µm. (C) Strain CCMP788, terminal cell. Note the claw-shaped TFPP ends and the long TRPP (arrow). Scale bar, 2 µm. (D) Strain SZN-B141, terminal valve with truncated TFPP ends and the long TRPP (arrow). Scale bar, 2 µm. (E) Strain CCMP788, intercalary valves with 1:1, knuckle-like IFPP junctions and IRPP (arrow). Scale bar, 2 µm. (F) Strain CCMP788, intercalary valves with 1:1 junctions. Scale bar, 2 µm. (G) Strain SZN-B141, detail of contiguous 1:2 junctions. Scale bar, 0.5 µm. (H) Strain SZN-B141, cingular band with rows of pores. Scale bar, 1 µm.

S. subsalsum. Relationships among the four lineages were unresolved.

The ML analyses with or without *Porosira pseudodenticulata and Lauderia annulata*, with or without *Detonula confervacea*, and with or without *Ditylum brightwellii*, *Lithodesmium undulatum*, *Helicotheca tamesis*, and *Bellerochea malleus* resulted in the same ML topology within *Skeletonema*. Therefore, we used *Thalassiosira pseudonana* Hasle et Heimdal and *Thalassiosira* sp. 1 as outgroups to calculate the ML bootstrap values for the clades within *Skeletonema*. These two taxa were always resolved as the nearest neighbors of *Skeletonema*.

The MP analysis resulted in a different topology among the ingroup taxa (data not shown). As in Figure

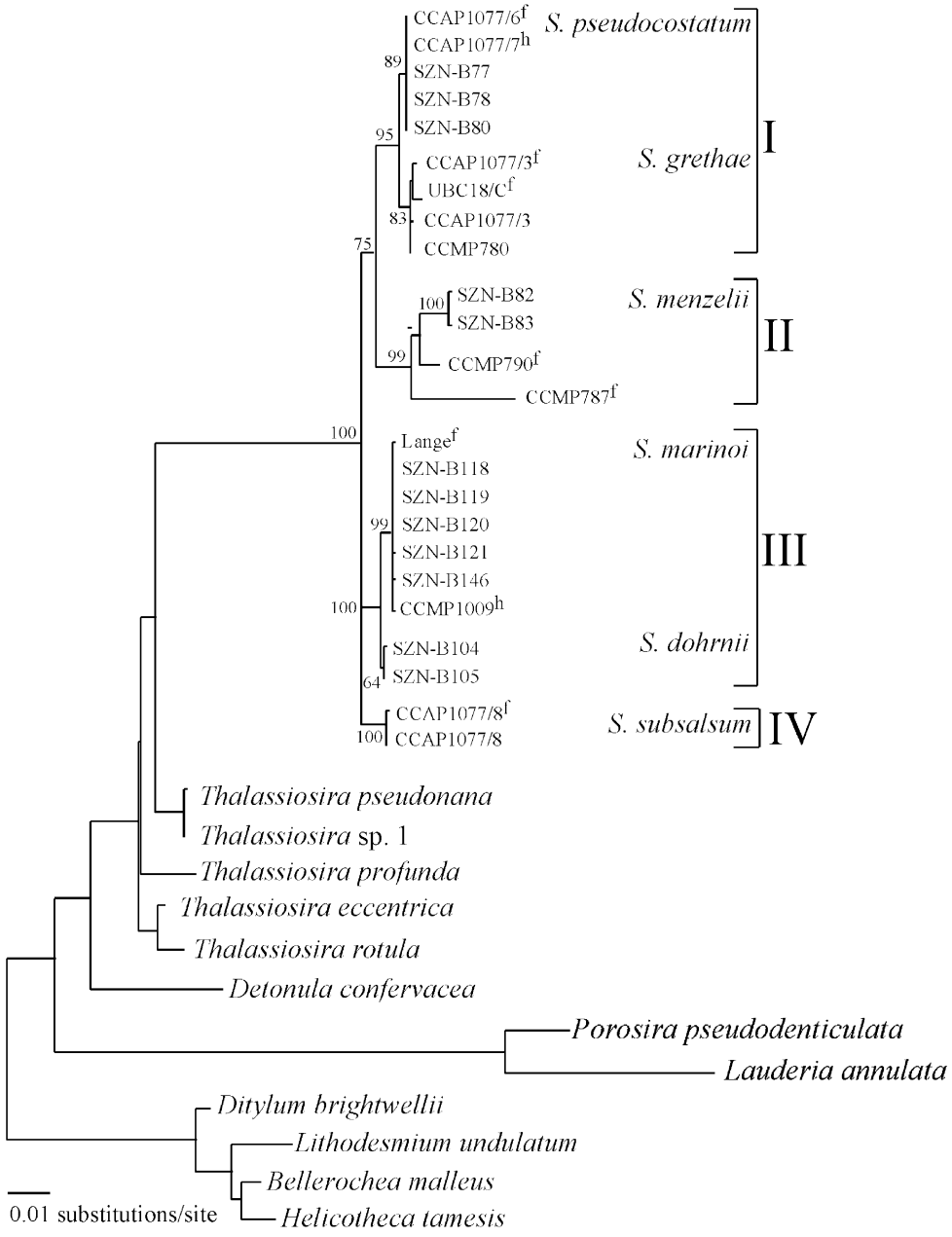

FIG. 10. ML tree ($-\ln L = 6385.3365$) inferred from the nuclear rDNA SSU of strains assigned to *Skeletonema* and other Thalassiosiraceae. *Ditylum brightwellii*, *Lithodesmium undulatum*, *Helicotheca tamesis*, and *Bellerochea malleus* have been chosen as outgroup. "f" denotes sequence downloaded from GenBank; "h" denotes sequence downloaded from GenBank, also sequenced at SZN with identical results (see Table 1). All the outgroup sequences are downloaded from GenBank.

10, *S. grethae* and *S. pseudocostatum* grouped together and so did *S. dohrnii* and *S. marinoi*, but the clade with *S. menzelii* diverged as the basal clade and *S. subsalsum* became sister to the clade with *S. dohrnii* and *S. marinoi*.

The 35 nuclear-encoded partial LSU rDNA sequences of *Skeletonema* aligned without problems into 785 positions. Ten distinct genotypes were recovered among the sequences. *Skeletonema* LSU sequences were subsequently aligned with ones from *Thalassiosira rotula* Meunier and *Thalassiosira* sp. 2 strain SZN-B101. Eleven extra gaps needed to be introduced, but the alignment among the *Skeletonema* sequences remained unaltered. The final alignment included 122 parsimony informative sites. Both hLRT and AIC tests selected a general time reversible model ($A \leftrightarrow C = 0.9493$, $A \leftrightarrow G = 1.9029$, $A \leftrightarrow T = 2.3025$, $C \leftrightarrow G = 0.8701$, $C \leftrightarrow T = 5.3265$ against $C \leftrightarrow T$ set at 1.0000) with unequal base composition ($A = 0.2591$, $C = 0.1999$, $G = 0.2902$, $T = 0.2508$), a proportion of invariable sites of 0.6281, and a gamma shape parameter of 1.8414 ($GRT + I + G$).

The ML tree inferred from the partial LSU sequences is presented in Figure 11. All species were monophyletic, and most of them were well resolved, though *S. dohrnii* obtained low support (63%) and *S. grethae* obtained no support at all. The latter lacked any synapomorphies among their LSU sequences. *Skeletonema tropicum* grouped with *S. pseudocostatum*, *S. grethae*, and *S. japonicum* in lineage I with high bootstrap support. Sequences of *S. menzelii* were recovered

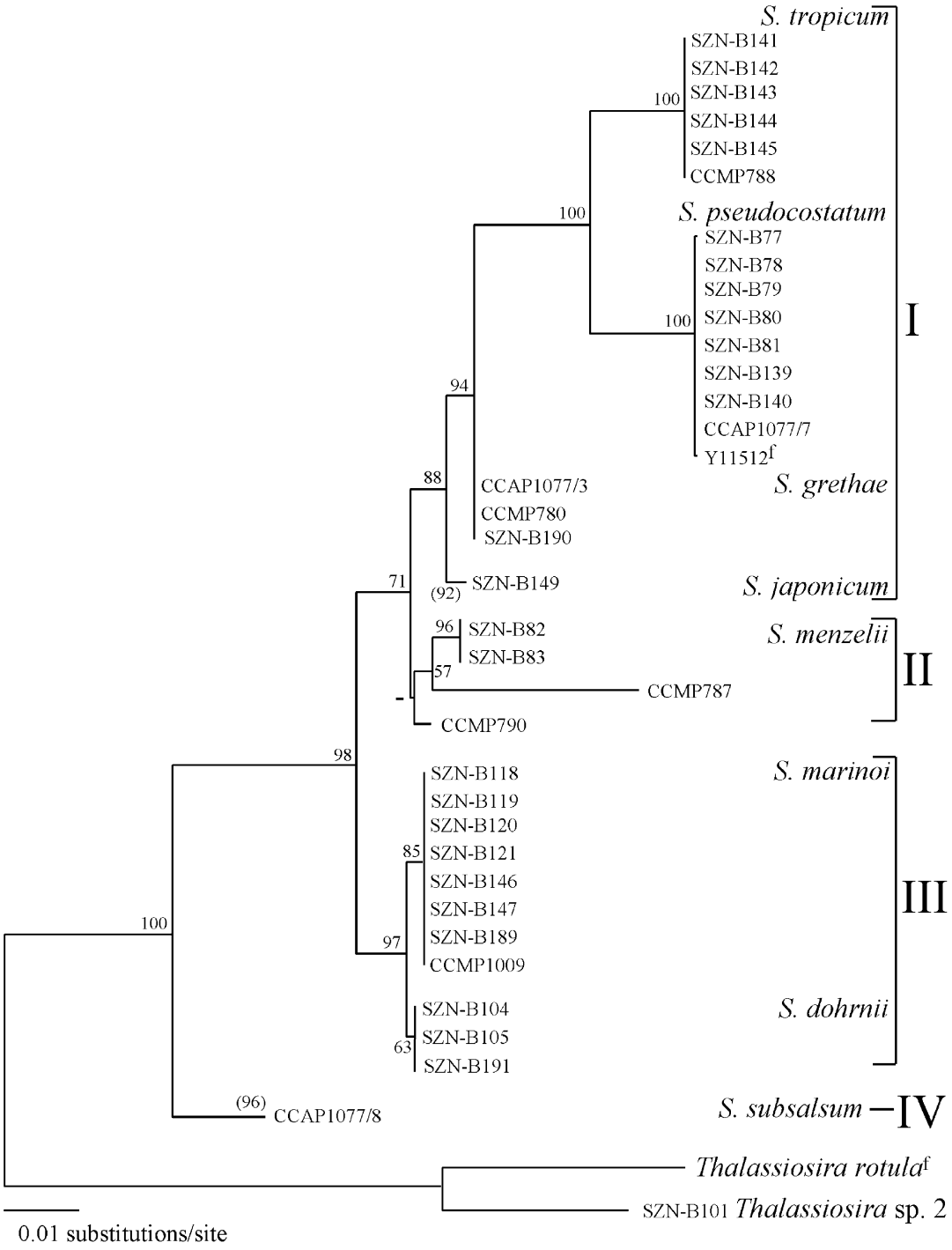

FIG. 11. ML tree (– ln L = 2214.1056) inferred from 785 positions at the 5 end of the nuclear rDNA LSU region of strains assigned to *Skeletonema* and two outgroup taxa belonging to *Thalassiosira*. "f" denotes sequences downloaded from GenBank (see Table 1). Bootstrap values in brackets have been generated duplicating the single sequence to the right.

in lineage II, the sister clade to lineage I. Sequences of *S. marinoi* and *S. dohrnii* were recovered in a well-supported lineage III, sister to the lineages I and II clade, and finally, the sequence of *S. subsalsum* was recovered as sole representative of lineage IV. The latter diverged first from the remainder of *Skeletonema*.

The SSU and LSU tree corroborated each other topologically. However, the SSU tree failed to resolve the basal ramification between lineages III and IV and the clade with lineages I and II, whereas the LSU tree did not recover any synapomorphies for *S. grethae*. In addition, both trees revealed considerable sequence

variation among the four strains of *S. menzelii*, with a comparable grouping pattern and associated branch lengths; for example, CCMP787 formed a long branch in both the SSU and LSU tree.

DISCUSSION

Species circumscription. The eight taxa examined in this study can be arranged into four main morphological groups, which correspond to the lineages I to IV identified in the phylogenetic tree. These groups are quite distinct from each other, whereas the interspecific differences within the groups are generally more subtle. Figure 12 shows the most informative morphological characters plotted on the ML phylogram inferred from the partial LSU sequences.

The four species in group I, *S. pseudocostatum*, *S. tropicum*, and the two new species, *S. grethae* and *S. japonicum*, share TFPPs with narrow distal ends and truncated, spiny, or claw-shaped margins. The distal parts of the IFPPs are also narrow in the fork-, knot-, and knuckle-like junctions, although they can be wider in the 1:2 junction mode in *S. tropicum* and *S. japonicum*. Within each species, a variable amount of silica is present in the junctions, generating further morphological variability.

The new species *S. grethae* was previously considered true *S. costatum* (Medlin et al. 1991), but a study of the type material of *S. costatum* (Zingone et al. 2005) contradicted this. In contrast to *S. grethae*, *S. costatum* is a robust species with closed and flattened IFPPs, 1:2 junctions with a zigzag connection line, claw-ended TFPPs, and a long RPP located marginally in all valves. *Skeletonema grethae* resembles instead a second morph found in the type material of *S. costatum*, which has been identified as a new species, *S. grevillei* Sarno et Zingone (Zingone et al. 2005). Like *S. grethae*, *S. grevillei* has TFPPs with narrow tips and truncated or spiny margins and 1:1, knuckle-like junctions. Nevertheless, *S. grevillei* has two distinctive features, a scallop-like ornamentation joining the bases of the FPPs and the TRP close to the ring of the TFPs, which discount any relationships with any known *Skeletonema* species.

Medlin et al. (1991) showed that *S. grethae* was distinct from *S. pseudocostatum* because its FPPs lack a tubular base. The present study shows that a tubular base is only present in the TFPPs of *S. pseudocostatum* and not in IFPPs. The IFPPs of *S. grethae* and *S. pseudocostatum* are indistinguishable. Medlin et al. (1991) could not compare the intercalary valves of the two species because their cultures of *S. pseudocostatum* did not form permanent chains.

The other new species in group I, *S. japonicum*, also has a tubular base to its TFPPs, like *S. pseudocostatum*. However, *S. japonicum* IFPPs interlock with fork joints, not intricate knuckles or knots, and are frequently of the 1:2 displaced type, with a clear zigzag at the level of the connection. In addition, *S. japonicum* is more robust than *S. pseudocostatum*, and the cingular bands have rows of relatively large pores. The last member of group I, *S. tropicum*, is the only examined *Skeletonema* with many chloroplasts. Its frustule is even more robust than that of *S. japonicum*. In addition, junctions in *S. tropicum* are always knot-like and the zigzag connection occasionally found in the Mediterranean strains of the species involves only a few IFPPs.

Group II only includes *S. menzelii*, which is uniquely noncolonial. The FPP ends are narrow as in group I and have two or three small spines. Another distinctive feature of *S. menzelii* is the delicate aspect of the frustule, which shows no areolae and very faint ribs on the bands. No major morphological differences were noted between Mediterranean strains and the original strain (Men 5 [CCMP787], Guillard et al. 1974). However, the regular 0.02-to 0.03-μm-diameter pores described for the latter were not seen in the cultures from the Gulf of Naples.

The other two new species, *S. marinoi* and *S. dohrnii*, are recovered in group III and differ from all other species in that their FPPs possess flat and flared tips with dentate margins. The intercellular junctions are apparently looser than those of the species in group I. They commonly show the 1:2 pattern with displaced IFPPs and a zigzag line along the whole connection between cells. The only morphological distinction between *S. marinoi* and *S. dohrnii* is the ultrastructure of the cingular bands.

Skeletonema subsalsum (group IV) contrasts with the other species: it has a thick frustule with a pseudoloculate structure and short tubular IFPPs. However, at higher salinities, >5.0 psu (Hasle and Evensen 1975, Paasche et al. 1975), the IFPPs may be longer. IFPPs of contiguous cells are displaced also in the 1:1 junction and are variable in shape, sometimes with lateral connections. Somewhat similar IFPPs are only found in *S. costatum*. As an example, the *S. subsalsum* specimen in figure 19 in Hasle and Evensen (1975) is rather similar to the *S. costatum* specimen shown in Figure 3G in Zingone et al. (2005). Furthermore, in *S. subsalsum* specimens with long IFPPs, the IRPP is long and adjoins the tips of two IFPPs of the sibling valve in the same fashion as in *S. costatum* (Zingone et al. 2005). However, no specimens of *S. costatum* in the type material show short IFPPs or a 1:1 junction type, which are frequently seen in *S. subsalsum*. The straight and narrow claw-shaped TFPPs of *S. costatum* also look quite different from the short and irregular ones of *S. subsalsum*. Finally, the TRP is subcentral in *S. subsalsum*.

Although subtle, some differences among these *Skeletonema* species can be seen with high quality LM, especially when equipped with Nomarski differential interference contrast. For example, the shape of TFPPs can be used to distinguish *S. dohrnii* and *S. marinoi* (with their flared TFPP tips, Fig. 1D) from *S. grethae*, *S. japonicum*, and *S. pseudocostatum* (with their narrow TFPP tips, Fig. 1F). Other species are even easier to recognize; for example, *S. tropicum* has numerous chloroplasts per cell (Fig. 9A), and *S. menzelii* always occurs as single cells or pairs of cells (Fig. 6A).

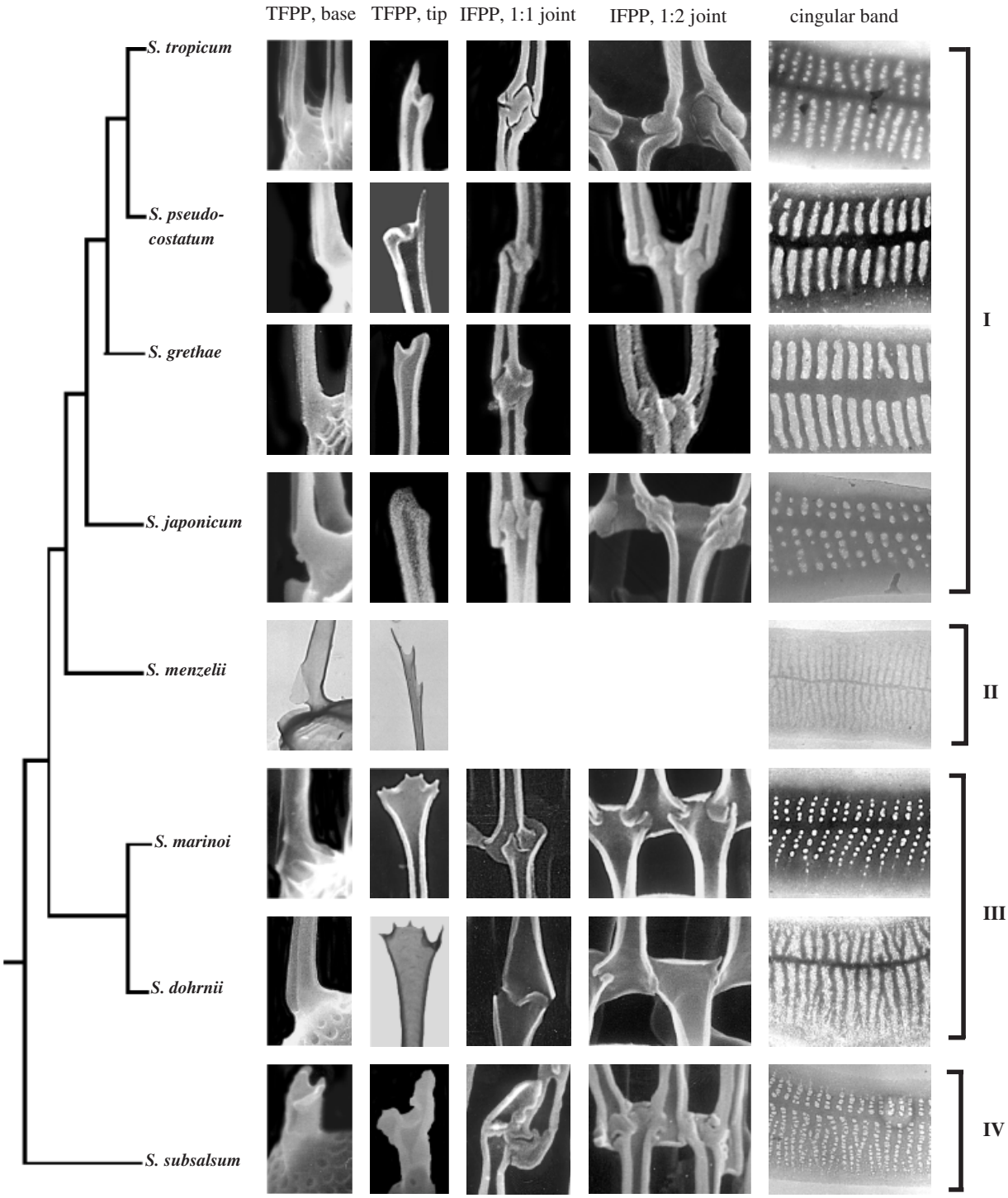

FIG. 12. State of TFPP shape (base and tip), IFPP junction (1:1 and 1:2), and cingular band ultrastructure of *Skeletonema* species plotted on the ML phylogram inferred from the LSU sequences.

Skeletonema potamos and *S. cylindraceum* have not been incorporated in this study because we had no access to live material. *Skeletonema potamos* (Hasle and Evensen 1976) is a freshwater species and is distinct from all other *Skeletonema* spp. because it possesses tubular FPPs, as observed in *S. subsalsum*, but with no apparent suture along their length. In addition, *S. potamos* IFPPs do not interlock with opposite IFPPs but simply abut against the sibling valve face, probably fusing with it. *Skeletonema cylindraceum* has been described from the Caspian Sea (Makarova and Proschkina-Lavrenko 1964). Like *S. tropicum*, this species possesses several

(3–12) chloroplasts per cell, but the morphological information provided in its description does not suffice to permit comparison with the species examined in the present study.

Phylogeny. Specimens belonging to the same morphologically circumscribed species share identical LSU sequences, and their SSU sequences are also similar or identical. Specimens belonging to morphologically distinct species possess distinct SSU and LSU sequences. The only case where this pattern does not apply is *S. menzelii*, which shows profound differences in LSU and SSU sequences among strains despite their similar morphology. However, detailed morphological analyses were not performed on this species in this study, which was focused on species diversity in *S. costatum*-like species. *Skeletonema menzelii* was added as a putative outgroup based on its distinct morphology, but rather unexpectedly, the phylogenies recovered it among the ingroup taxa. The significance of the molecular differences found among *Skeletonema* species is generally high, as for example in the case of the SSU rDNA sequences of *S. pseudocostatum* and *S. grethae*, which show compensatory base changes (Medlin et al. 1995).

Because of their topological agreement, the trees inferred from the SSU and LSU sequences probably reflect cladogenesis within the genus. The SSU tree fails to resolve the basal ramification of *Skeletonema* and the LSU tree lacks synapomorphies for *S. grethae*, but the four lineages are recovered in both of them, as are the sister relationships between lineages I and II. However, the similar outcome of the trees can be partly explained by the proximity of SSU and LSU in rDNA cistrons. Phylogenies inferred from unrelated DNA regions, preferably from mitochondria and plastids, are needed to confirm patterns revealed by ribosomal genes. Unfortunately, the interspecific comparison remains incomplete because the SSU of *S. tropicum* and *S. japonicum* failed to amplify. This could be because of inserts in the SSU, which can thwart direct PCR amplification of this region. Failure to amplify the SSU region in *S. tropicum* strains could be viewed as a taxon-defining character in its own behalf because it occurred in all strains of this species that we tested.

Our results confirm the conclusion that *S. grethae* (as *S. costatum*) and *S. pseudocostatum* are different species (Medlin et al. 1991) because the sequence difference in the SSU gene region is corroborated by much more conspicuous differences along the LSU region. In addition, several additional strains of *S. pseudocostatum* all share identical SSU and LSU sequences. This study also found that *S. tropicum* is more closely related to *S. pseudocostatum* than to *S. grethae*. Although *S. dohrnii*, *S. grethae*, *S. japonicum*, *S. marinoi*, and *S. pseudocostatum* were formerly treated as *S. costatum*, they do not group together. Morphologically distinct species, such as *S. tropicum* and *S. menzelii* are recovered with the former "*S. costatum*" strains, and the features by which they differ from the general "*S. costatum*" morphology, that is, the presence of multiple chloroplasts and the solitary habit, are evolutionary novelties.

Assessment of the phylogenetic value of morphological characters. An analysis of the distribution of morphological characteristics along the LSU tree of *Skeletonema* species (Fig. 12) permits the recognition of five groups of characters of different phylogenetic value. This analysis can only be provisional because as new species and character states are discovered, the pattern may change.

The first category includes a single character showing shared derived states (synapomorphies), that is, the width of the distal parts of TFPPs, which has acquired the state "narrow" in the clade with the lineages I and II and the state "wide" in lineage III (*S. marinoi* and *S. dohrnii*). The second category includes characters that also change state only once, but their derived states delimit only single species. Examples are the occurrence of multiple chloroplasts in *S. tropicum*, the absence of colonies in *S. menzelii*, and the tubular IFPPs in *S. subsalsum*. Such states do not contribute to our understanding of the evolution of the genus, but they are relevant from a taxonomic viewpoint because they are diagnostic for species.

The third set contains characters that also show more or less discrete states, but they reveal multiple acquisitions and/or secondary losses. For instance, the character "shape of the basal parts of the TFPPs" changes at least twice. The state "tubular in the basal part" could have been acquired at the branch leading to lineage I but was then lost secondarily in *S. grethae*. Alternatively, it may have been acquired independently twice: once in *S. japonicum* and once along the branch to *S. tropicum* and *S. pseudocostatum*. The character "ultrastructure of the bands" shows an even more complex pattern of state changes with several alternative explanations for acquisitions and secondary losses of the row of pores between ribs in the copulae. As in the case of the second category, such characters do not really help in the reconstruction of the evolutionary history of the genus, but they are informative from a taxonomic viewpoint and help define a species.

The fourth category of characters includes most morphometric parameters, for example, the number of cells per colony, valve diameter, number of FPs per valve, which show considerable variation both among and within species, ranges often overlapping between species (Tables 2 and 3), as already noted by Hasle (1973). Such characters are neither phylogenetically nor systematically informative, though extreme values can help in the identification of single species. The poor diagnostic value of gross morphology is predictable, because size reduction accompanying the vegetative cell cycle profoundly influences cell outlines (Round et al. 1990) and other features that depend on size, for example, the number of FPPs per valve. Perhaps some of these characters may prove to be informative if they are analyzed with geometric morphometrics (unpublished data). In *Cyclotella meneghiniana*, certain features, such as the tilt and the size of the FP

TABLE 3. Main morphological characters distinguishing *Skeletonema* species.

Species	Chloroplasts	Satellite pores	TFPP			IFPP joints[a]	IRP	Cingular band ultrastructure
			shape	Tip width	Tip shape			
S. dorhnii	1–2	3	Split tube	Flared	Dentate	1:2	Short	Hyaline areas
S. grethae	1–2	3	Split tube	Narrow	Claw-like, truncated, or spiny	1:1	Short	Hyaline areas
S. japonicum	1–4	3	Close at the base	Narrow	Truncated or claw-like	1:2	Short	Rows of pores
S. marinoi	1–2	3	Split tube	Flared	Dentate	1:2	Short	Rows of pores
S. menzelii	1–2	2	Split tube	Narrow	Spiny	—		Hyaline areas
S. pseudocostatum	1–2	3	Close at the base	Narrow	Claw-like, truncated, or spiny	1:1	Short	Hyaline areas
S. subsalsum	1–2	3	Close with a pore	Narrow	Hook-like	1:2	Long	Rows of pores
S. tropicum	1–7	3	Split tube	Narrow	Claw-like or truncated	1:2	Short	Rows of pores

All information is from culture material.

[a]1:2 includes only cases when 1:2 connections are found in contiguous junctions. All 1:1 can occasionally form isolated 1:2 joints.

tube, were recovered by the geometric morphometric analysis as being phylogenetically informative (unpublished data).

A fifth set of characters shows scarcely any variability in *Skeletonema* species. Examples are the states such as "number and spatial density of areolae," "spatial density of FPPs," and "density of ribs in cingular bands," which vary little among *Skeletonema* species. In contrast, some of these characters are variable and diagnostic for species in the genus *Thalassiosira*.

Not only morphometric but also ultrastructural features of the frustule mentioned above are susceptible to intraspecific variation. One example is the shape of the TFPPs, which in *S. grethae* and *S. tropicum* can either be truncated distally or end with a claw-like or a spiny protrusion. Another example are the cingular bands in *S. dohrnii*, which generally have hyaline areas between ribs but show rows of pores in a few specimens from culture material. Although observations were performed on many specimens, the whole range of variability of these characters still needs to be understood fully. Several characters have already been shown to vary under the influence of environmental factors. As an example, *S. pseudocostatum* was found to grow only as single cells in previous observations (Medlin et al. 1991), possibly because of the use of a very enriched culture medium, with soil extract. Also in natural samples from the Gulf of Naples, this species is generally recorded as single cells during the late spring–summer blooms (Ribera d'Alcalà et al. 2004). Another example is the length of the IFPPs in *S. subsalsum*, which varies in relation to salinity and osmotic pressure values (Paasche et al. 1975). However, these ultrastructural features generally do not show overlapping ranges in their states. Therefore, in contrast to characters in the fourth category, those in the fifth retain phylogenetic and/or taxonomic value despite their observed variability.

Ecology. The distribution of the species identified in this study provides, in some cases, evidence of distinct ecological characteristics. The four *Skeletonema* species found in the Gulf of Naples tend to occupy different seasonal niches: *S. dohrnii* has only been found in winter, *S. pseudocostatum* blooms in late spring, early summer, *S. tropicum* is recorded in late summer, early autumn, and *S. menzelii* is typical of autumn. These periods are characterized by markedly different conditions in terms of temperature (13–30° C), salinity (25–38 psu), water column stability, photoperiod, and nutrient concentrations (Ribera d'Alcalà et al. 2004). It is hence conceivable that the four species have different ecological requirements. Distributional differences in relation to the rainy season and the brackish conditions have also been shown for four distinct *Skeletonema* species (*S. tropicum*, *S. pseudocostatum*, *S. subsalsum*, and "*S. costatum*") in a tropical coastal lagoon in the Gulf of Mexico (Aké Castillo et al. 1995).

Skeletonema costatum sensu lato has been recorded from coastal areas all over the world and was hence considered a ubiquitous species. In contrast, the new species recognized within "*S. costatum*" does not seem to be ubiquitous. *Skeletonema dohrnii* is found in the Gulf of Naples and not in the Adriatic Sea, whereas the closely related species *S. marinoi*, which is abundant in the Adriatic Sea, has not been found in the Gulf of Naples. Nor has *S. pseudocostatum* been recorded in the Adriatic Sea so far, despite its abundance in the Gulf of Naples. This peculiar geographic distribution parallels seasonal patterns of occurrence in suggesting differences in the ecological requirements of the distinct species. On the other hand, even in our limited data set, some species already show a wide geographic range. For instance, *S. marinoi* was found in such distant places as Hong Kong Bay and the Adriatic Sea, whereas *S. peudocostatum* has been recorded in the Australian region and at Mediterranean sites. This is not surprising, because similar ecological conditions are often encountered in geographically separate areas. The coverage of our data set is far from extensive enough to make any firm statement on the actual biogeography and ecology of the distinct *Skeletonema*

species at this stage. On the other hand, the relevance of spatial and temporal patterns of *Skeletonema* species to ecological research warrants a closer examination of many strains over the seasonal cycle across the geographic range of the "*Skeletonema costatum*" species complex.

Toward a consensus species concept in Skeletonema. The circumscription of the species recognized within *Skeletonema* complies with the "consensus species concept." Indeed, morphologically distinct specimens are also genetically distinct, and genetically identical specimens generally exhibit a highly similar morphology. Differences observed in distribution and seasonality provide indications that *Skeletonema* species also have distinct ecological requirements, concurring with other data in the separation of taxa. Within the species complex once perceived as "*Skeletonema costatum*," there are cases of very clear distinction among species for morphological, phylogenetic, and ecological traits. As an example, *S. marinoi* and *S. pseudocostatum* are well separated from the molecular point of view, have distinct morphological traits, and also occur in different areas and seasons of the year, at least in the Mediterranean. Even *S. marinoi* and *S. dohrnii*, which only show subtle morphological differences, are separated from the molecular point of view and show a distinct occurrence in Italian Seas.

The biological species concept was not tested in this study. The only *Skeletonema* species analyzed so far (named *S. costatum* but showing many chloroplasts as *S. tropicum*) proved to be monoecious (Migita 1967), which makes cross-fertilization tests difficult to perform. In addition, vegetative enlargement (Gallagher 1983) prevents the use of size as a cue for sexual reproduction. These limitations warrant the use of specific molecular tools to verify gamete fusion between different strains and the fecundity of their offspring. Nevertheless, our results reveal, albeit indirectly, that the taxa are reproductively isolated entities. If they interbred freely with one another and if their offspring were perfectly viable, then they would neither show conspicuous morphological and genetic differences nor any correlation between morphology and sequence data. Moreover, one would not expect the large SSU differences among the various clades and compensatory base changes between sequences in different clades (Medlin et al. 1995).

High diversity within *Skeletonema* was detected for the first time by Gallagher (1980, 1982) based on significant differences in allozyme patterns among series of "*Skeletonema costatum*" strains collected in the summer and winter blooms in Narragansett Bay. In addition, Gallagher and coworkers (Gallagher 1982, Gallagher et al. 1984) demonstrated that strains exhibiting markedly different allozyme patterns also behaved differently under a series of experimental conditions; for example, summer bloomers grew faster in summer conditions (20° C) than in winter ones. These authors first concluded that blooms in Narragansett Bay were composed of different *Skeletonema* species or even different assemblages of species. In later studies, however, the genetic distinction between bloom periods tended to collapse with increasing numbers of individuals because intermediate allozyme patterns were encountered. Gallagher (1994) then concluded that distinct allozyme patterns were extremes in the cline of a single genetically diverse species. Our results indicate that the earlier conclusion (Gallagher 1982, Gallagher et al. 1984) was probably correct and that different species occur in Narragansett Bay at different seasons. The shared bands observed by Gallagher (1994) might either represent ancestral alleles present in sister species or result from incidental interspecific hybridization. Even if hybridization occurred and the hybrids were able to grow and divide clonally, then it would remain to ascertain whether such hybrids can reproduce sexually. Incidental hybridization may in itself constitute an effective mode of speciation (Veron 1995, Van Oppen et al. 2001, Vollmer and Palumbi 2002), but its occurrence does not preclude the possibility that we are dealing with distinct species.

Concluding remarks. The results of this research showed that the easily recognizable and ubiquitous "*S. costatum*" consists of distinct species. The startlingly high diversity has been observed in a restricted number of strains from a small part of the known geographic range of "*S. costatum*." Hence, it is conceivable that more *Skeletonema* species remain to be detected. Nonetheless, the present findings have significant implications for the diversity, phylogeny, and ecology of this important group of coastal marine phytoplankton as well as for the practical identification of *Skeletonema* species in natural samples.

One of the consequences of the fact that *S. costatum* is composed of several new species is that ecological and physiological information obtained in various studies on "*S. costatum*" must be reinterpreted. Different outcomes may not only result from different experimental designs or ecological conditions but also from taxonomic differences. Identification is still possible if experiments have been carried out on strains maintained in culture collections or records of *Skeletonema* species are accompanied by clear morphological information. For example, the Norwegian *Skeletonema* specimens in Hasle (1973) are similar to *S. marinoi*, whereas some Mediterranean strains in Castellví (1971) show the morphological features typical for *S. pseudocostatum*. However, at present the results presented here may have a limited relevance to the identification of *Skeletonema* species from other areas. More information on variability is needed before species can be identified reliably based on only morphology. Nevertheless, there is evidence that not all the species are ubiquitous or perennial. It is therefore likely that local identification keys will be built once that complete information on single areas is gathered. rRNA probes are being developed for each of the new species here plus *S. pseudocostatum* in hopes

of elucidating the true distribution of these species. rRNA probes can be applied to Lugol and formalin preserved material so archived material can be reanalyzed.

It has been postulated that marine microalgal species diversity is very low, compared with higher plants, and that many species are ubiquitous and ecologically plastic. Indeed, the lack of transport barriers in the aquatic environments apparently offers ample opportunity for huge numbers of small organisms to be transported from one site to another (Finlay and Clarke 1999, Finlay 2002). However, if apparently well-defined species consist of several genetically, biologically, and ecologically distinct species, this concept must be reexamined. The results of this investigation, as well as those on other marine microalgae such as *Phaeocystis* (Medlin et al. 1994, Zingone et al. 1999), *Scrippsiella* (Montresor et al. 2003), and *Pseudo-nitzschia* (Lundholm et al. 2003, Orsini et al. 2004), reveal surprisingly high diversity within taxa known to microalgal taxonomists for more than a century. Considering that other species have been studied less and/or never cultured, whereas yet more are still being discovered, a more cautious approach to defining phytoplankton diversity is highly recommended.

We are grateful to Gandi Forlani, Gennaro Iamunno, and Franco Iamunno for their skillful assistance with EM preparations. Thanks are also due to Carmen Minucci for help with the cultivation of *Skeletonema* strains. Paul Hargraves, Shin Uye, and Ken T. M. Wong graciously provided the strains of *S. grethae* from Florida, *S. japonicum* from Japan, and *S. marinoi* from China, respectively. Antonio Miralto and Cecilia Totti kindly provided samples from the Adriatic Sea. Maria Pia Zingone is acknowledged for the revision of the Latin diagnoses of the new species. L. K. M. wishes to acknowledge Anne Hervé, who first drew her attention to the fact the cell of the *S. pseudocostatum* genotype could make permanent colonies. This project was stimulated by information gathered in the Italian project MURST-SINAPSI and funded by SZN, Naples.

Aké Castillo, J., Meave del Castillo, M. E. & Hernández-Becerril, D. U. 1995. Morphology and distribution of species of the diatom genus *Skeletonema* in a tropical coastal lagoon. *Eur. J. Phycol.* 30:107–15.

Anonymous. 1975. Proposals for a standardization of diatom terminology and diagnoses. *Nova Hedw. Beih.* 53:323–54.

Bernardi Aubry, F., Berton, A., Bastianini, M., Socal, G. & Acri, F. 2004. Phytoplankton succession in a coastal area of the NW Adriatic, over a 10-year sampling period (1990–1999). *Cont. Shelf. Res.* 24:97–115.

Castellví, J. 1971. Contribución a la biología de *Skeletonema costatum* (Grev.). *Invest. Pesq.* 35:365–520.

Cleve, P. T. 1873. Examination of diatoms found on the surface of the sea of Java. *Bih. Kongl. Svenska Vetensk.-Akad. Handl.* 11: 3–13.

Cleve, P. T. 1900. Notes on some Atlantic plankton-organisms. *Kongl. Svensk Vetensk.-Akad. Handl.* 34:3–22.

Cloern, J. E., Cole, B. E., Wong, R. L. J. & Alpine, A. E. 1985. Temporal dynamics of estuarine phytoplankton: a case study of San Francisco Bay. *Hydrobiologia* 129:153–76.

Estrada, M., Vives, F. & Alcaraz, M. 1985. Life and the productivity of the open sea. *In* Margalef, R. [Ed.] *Western Mediterranean*. Pergamon Press, Oxford, UK, pp. 148–97.

Finlay, B. J. 2002. Global dispersal of free-living microbial eukaryote species. *Science* 296:1061–3.

Finlay, B. J. & Clarke, K. J. 1999. Ubiquitous dispersal of microbial species. *Nature* 400:323.

Fryxell, G. A. 1976. The position of the labiate process in the diatom genus *Skeletonema*. *Br. Phycol. J.* 11:93–9.

Gallagher, J. C. 1980. Population genetics of *Skeletonema costatum* (Bacillariophyceae) in Narragansett Bay. *J. Phycol.* 16:464–74.

Gallagher, J. C. 1982. Physiological variation and electrophoretic banding patterns of genetically different seasonal populations of *Skeletonema costatum* (Bacillariophyceae). *J. Phycol.* 18: 148–62.

Gallagher, J. C. 1983. Cell enlargement in *Skeletonema costatum* (Bacillariophyceae). *J. Phycol.* 19:539–42.

Gallagher, J. C. 1994. Genetic structure of microalgal populations. I. Problems associated with the use of strains as terminal taxa. *In* Kociolek, J. P. [Ed.] *Proceedings of the 11th International Diatom Symposium 1990*. California Academy of Sciences, San Francisco, CA, pp. 69–86.

Gallagher, J. C., Wood, A. M. & Alberte, R. S. 1984. Ecotypic differentiation in the marine diatom *Skeletonema costatum*: influence of light intensity on the photosynthetic apparatus. *Mar. Biol.* 82:121–34.

Greville, R. K. 1866. Description of new and rare diatoms. Series 20. *Trans. Micr. Soc. London, n. s.* 14:77–86.

Guillard, R. R. L. 1975. Culture of phytoplankton for feeding marine invertebrates. *In* Smith, W. L. & Chanley, M. H. [Eds.] *Culture of Marine Invertebrate Animals*. Plenum Press, New York, pp. 29–60.

Guillard, R. R. L., Carpenter, E. J. & Reimann, B. E. F. 1974. *Skeletonema menzelii* sp. nov., a new diatom from the western Atlantic Ocean. *Phycologia* 13:131–8.

Hasle, G. R. 1973. Morphology and taxonomy of *Skeletonema costatum* (Bacillariophyceae). *Norw. J. Bot.* 20:109–37.

Hasle, G. R. 1978. Diatoms. *In* Sournia, A. [Ed.] *Phytoplankton Manual*. UNESCO, Paris, pp. 136–42.

Hasle, G. R. & Evensen, D. L. 1975. Brackish-water and fresh-water species of the diatom genus *Skeletonema* Grev. I. *Skeletonema subsalsum* (A. Cleve) Bethge. *Phycologia* 14:283–97.

Hasle, G. R. & Evensen, D. L. 1976. Brackish water and fresh water species of the diatom genus *Skeletonema*. II. *Skeletonema potamos* comb. nov. *J. Phycol.* 12:73–82.

Housley, H. L., Scheetz, W. & Pessoney, G. F. 1975. Filament formation in the diatom *Skeletonema costatum*. *Protoplasma* 86: 363–9.

Hulburt, E. M. & Guillard, R. R. L. 1968. The relationship of the distribution of the diatom *Skeletonema tropicum* to temperature. *Ecology* 49:337–9.

Karentz, D. & Smayda, T. J. 1984. Temperature and seasonal occurrence patterns of 30 dominant phytoplankton species in Narragansett Bay over a 22-year period (1959–1980). *Mar. Ecol. Prog. Ser.* 18:277–93.

Kooistra, W. H. C. F., De Stefano, M., Medlin, L. K. & Mann, D. G. 2003. The phylogenetic position of *Toxarium*, a pennate-like lineage within centric diatoms (Bacillariophyceae). *J. Phycol.* 39:185–97.

Lundholm, N., Moestrup, Ø., Hasle, G. R. & Hoef-Emden, K. 2003. A study of the *Pseudo-nitzschia pseudodelicatissima/cuspidata* complex (Bacillariophyceae): what is *P. pseudodelicatissima*? *J. Phycol.* 39:797–813.

Makarova, I. V. & Proschkina-Lavrenko, A. I. 1964. Diatomeae novae e Mari Caspico. *Nov. Syst. Plant. Non Vasc.* 1:34–43.

Medlin, L. K., Elwood, H. J., Stickel, S. & Sogin, M. L. 1991. Morphological and genetic variation within the diatom *Skeletonema costatum* (Bacillariophyta): evidence for a new species, *Skeletonema pseudocostatum*. *J. Phycol.* 27:514–24.

Medlin, L. K. & Kaczmarska, I. 2004. Evolution of the diatoms: V. Morphological and cytological support for the major clades and a taxonomic revision. *Phycologia* 43:245–70.

Medlin, L. K., Kooistra, W. C. H. F. & Schmid, A.-M. M. 2000. A review of the evolution of the diatoms—a total approach using molecules, morphology and geology. *In* Witkowski, A. & Sieminska, J. [Eds.] *The Origin and Evolution of the Diatoms: Fossil Molecular and Biogeographical Approaches*. W. Szafer

Institute of Botany, Polish Academy of Science, Cracow, pp. 13–35.
Medlin, L. K., Lange, M., Barker, G. L. A. & Hayes, P. K. 1995. Can molecular techniques change our ideas about the species concept? *In* Joint, I. [Ed.] *Molecular Ecology of Aquatic Microbes*. Springer-Verlag, Berlin, pp. 133–52.
Medlin, L. K., Lange, M. & Baumann, M. E. M. 1994. Genetic differentiation among three colony-forming species of *Phaeocystis*: further evidence for the phylogeny of the Prymnesiophyta. *Phycologia* 33:199–212.
Migita, S. 1967. Sexual reproduction of centric diatom *Skeletonema costatum*. *Bull. Jpn. Soc. Sci. Fish.* 33:392–8.
Montresor, M., Sgrosso, S., Procaccini, G. & Kooistra, W. H. C. F. 2003. Intraspecific diversity in *Scrippsiella trochoidea* (Dinophyceae): evidence for cryptic species. *Phycologia* 42:56–70.
Orsini, L., Procaccini, G., Sarno, D. & Montresor, M. 2004. Multiple rDNA ITS-types within the diatom *Pseudo-nitzschia delicatissima* (Bacillariophyceae) and their relative abundances across a spring bloom in the Gulf of Naples. *Mar. Ecol. Prog. Ser.* 271:87–98.
Orsini, L., Sarno, D., Procaccini, G., Poletti, R., Dahlmann, J. & Montresor, M. 2002. Toxic *Pseudo-nitzschia multistriata* (Bacillariophyceae) from the Gulf of Naples: morphology, toxin analysis and phylogenetic relationships with other *Pseudo-nitzschia* species *Eur. J. Phycol.* 37:247–57.
Paasche, E., Johansson, S. & Evensen, D. L. 1975. An effect of osmotic pressure on the valve morphology of the diatom *Skeletonema subsalsum*. *Phycologia* 14:205–11.
Posada, D. & Crandall, K. A. 2001. Selecting the best-fit model of nucleotide substitution. *Syst. Biol.* 50:580–601.
Ribera d'Alcalà, M., Conversano, F., Corato, F., Licandro, P., Mangoni, O., Marino, D., Mazzocchi, M. G., Modigh, M., Montresor, M., Nardella, M., Saggiomo, V., Sarno, D. & Zingone, A. 2004. Seasonal patterns in plankton communities in a pluriannual time series at a coastal Mediterranean site (Gulf of Naples): an attempt to discern recurrences and trends. *Sci. Mar.* 68(suppl 1):65–83.
Ross, R., Cox, E. J., Karayeva, N. I., Mann, D. G., Paddock, T. B. B., Simonsen, R. & Sims, P. A. 1979. An amended terminology for the siliceous components of the diatom cell. *Nova Hedw. Beih.* 64:513–33.
Ross, R., Sims, P. A. & Gallagher, J. C. 1996. Proposals to conserve the names *Skeletonema* Grev., with a conserved type, and *Skeletonemopsis* P.A. Sims (*Bacillariophyceae*). *Taxon* 45:315–6.
Round, F. E. 1973. On the diatom genera *Stephanopyxis* Ehr. and *Skeletonema* Grev. and the classification in a revised system of the Centrales. *Bot. Mar.* 16:148–54.
Round, F. E., Crawford, R. M. & Mann, D. G. 1990. *The Diatoms. Biology and Morphology of the Genera*. Cambridge University Press, Cambridge, 747 pp.
Sims, P. A. 1994. *Skeletonemopsis*, a new genus based on the fossil species of the genus *Skeletonema* Grev. *Diatom Res* 9:387–410.
Smith, M. A. 1981. The frustular and cytoplasmic fine structure of vegetative cells of *Skeletonema costatum* (Greville) Cleve. *Bacillaria* 4:223–40.
Swofford, D. L. 2002. *PAUP*-Phylogenetic Analysis Using Parsimony (*And Other Methods)*. Version 4.0b10. Sinauer Associates, Sunderland, Massachusetts.
Totti, C. M., Cucchiari, E. M. & Romagnoli, T. 2002. Variazioni intra e interannuali del fitoplancton nell'area costiera di Senigallia (Adriatico settentrionale) dal 1988 al 2000. *Biol. Mar. Med.* 9:391–9.
Van Oppen, M. J. H., McDonald, B. J., Willis, B. & Miller, D. J. 2001. The evolutionary history of the coral genus *Acropora* (Scleractinia, Cnidaria) based on a mitochondrial and a nuclear marker: reticulation, incomplete lineage sorting, or morphological convergence? *Mol. Biol. Evol.* 18:1315–29.
Veron, J. E. N. 1995. *Corals in Space and Time: the Biogeography and Evolution of the Scleractinia*. Cornell University Press, Ithaca, NY, 321 pp.
Vollmer, S. V. & Palumbi, S. R. 2002. Hybridization and the evolution of reef coral diversity. *Science* 296:2023–5.
Yamada, M. & Takano, H. 1987. Thin fibres emitted by the marine diatom *Skeletonema costatum* (Grev.) Cleve. *Bull. Tokai fish. Res. Lab.* 121:35–9.
Zingone, A., Chrétiennot-Dinet, M.-J., Lange, M. & Medlin, L. 1999. Morphological and genetic characterization of *Phaeocystis cordata* and *Phaeocystis jahnii* (Prymnesiophyceae), two new species from the Mediterranean Sea. *J. Phycol.* 35:1322–37.
Zingone, A., Percopo, I., Sims, P. A. & Sarno, D. 2005. Diversity in the genus *Skeletonema* (Bacillariophyceae). I. A reexamination of the type material of *S. costatum* with the description of *S. grevillei* sp. nov. *J. Phycol.* 41:000–000.
Zoppini, A., Pettine, M., Totti, C., Puddu, A., Artegiani, A. & Pagnotta, R. 1995. Nutrients, standing crop and primary production in western coastal waters of the Adriatic Sea. *Estuar. Coast. Shelf Sci.* 41:493–513.